

---

## A GAN “STEERABILITY” WITHOUT OPTIMIZATION: APPENDIX

### A.1 QUANTITATIVE EVALUATION

We adopt the method proposed in Jahanian et al. (2020) and utilize the *MobileNet-SSD-V1* detector<sup>2</sup> to estimate object bounding boxes. To quantify shifts, we extract the centers of the bounding boxes along the corresponding axis. To quantify zoom, we use the area of the bonding boxes. In the following paragraphs, we elaborate on all quantitative evaluations reported in the main text.

**Figure 4** Here, we show the probability densities of object areas and locations after 2 (top) and 5 (bottom) steps. Since we use unit-norm direction vectors, the length of the linear paths we walk through are 2 and 5 as well. As for the nonlinear path, we choose the first step to have the same length. However, the overall length of the path is different. For example, on average, five steps of the nonlinear trajectory have a total length of 5.95, but reach at a point of distance only 4.3 from the initial point. We used 100 randomly chosen classes from the ImageNet dataset, and 30k images from each class. The same images are used for both the FID measurement and for generating the PDF plots.

**Figure 6** In order to ensure that each step of the linear walk and the great and small circle walks has the same geodesic distance, we set

$$\Delta_L = \Delta_G \|z_0\| = \Delta_S \|\mathbf{P}_V z_0\|, \quad (12)$$

where  $\Delta_L$ ,  $\Delta_G$  and  $\Delta_S$  are the step sizes of the linear, great circle and small circle walks, respectively. This ensures that the arc-length of a step on the circles is the same as the length of a step of the linear walk.

**Figure 7** Here, we aim to demonstrate a particular second order dataset bias. We chose 10 classes which we found to exhibit strong coupling between the size and location of the object. For example, dogs, cats and in general, animals. We plotted 80 levels-sets of 2D KDEs computed using the *seaborn* package. In Fig. 7 we show results for a Labrador retriever dog, we observed similar results for the classes: golden retriever (207), Welsh springer spaniel (218), Great grey Owl (24), Persian cat (283), plane (726), tiger (292), Old English sheepdog (229), passenger car (705), goose (99), husky (248). See Figs. 40 and 41 for additional results.

**Table 1** In Tab. 1, we compare the running time and memory usage of all methods. For<sup>3</sup> (Jahanian et al., 2020), we measure the time it takes to learn one direction, which includes the training process. For<sup>4</sup> (Härkönen et al., 2020), we measure the total time it takes to extract the directions, including the sample collection, the PCA, and the regression. We noticed that the regression stage was the heaviest. As for our method, we measure the time it takes the CPU to perform SVD. The column “Memory” specifies the required memory for collecting samples. Only GANSpace (Härkönen et al., 2020) requires that stage.

### A.2 UNSUPERVISED EXPLORATION OF PRINCIPAL DIRECTIONS

#### A.2.1 COMPARISONS WITH RANDOM DIRECTIONS

In Fig. 10 - 9 we explore principal directions via linear walks, using the same initial image (in the middle). In Figs. 14-16 we explore the transformations that arise in each hierarchy of BigGAN-128. Specifically, we compare our linear directions which are based on SVD, with random directions. We draw 5 different directions from an isotropic Gaussian distribution and normalize them to have unit-norms, similarly to our directions. Then, we linearly add them to the initial latent code with fixed number of steps. We can observe that each random direction induces a different complex effect, which cannot be described by a single semantic property. For examples, in the first random direction (R1) we can see rotation, zoom and background changes, while in the third (R3), there is a kind of vertical shift. On the other hand, our principal directions show one prominent transformation

<sup>2</sup><https://github.com/qfgaoqiao/pytorch-ssd>

<sup>3</sup><https://github.com/ali-design/>

<sup>4</sup><https://github.com/harskish/ganspace/>

---

for each scale. We focus on directions that have the same effect for all classes and do not show directions that lead to different effects for different classes, like changes of day-night in one class and background in another class.

### A.2.2 ALTERNATIVE SMALL CIRCLE WALKS

In Figs. 29-33, we show more examples, this time with small circle walks towards principal directions. In all those examples, the reference direction  $v_{\text{ref}}$  for the small circle, is the least dominant direction (namely, the singular vector with the smallest singular value). This ensures that when walking towards the principal direction  $v$ , we modify no other dominant property. That is, we modify the property associated with  $v$  without modifying the properties associated with any other principal direction, besides  $v_{\text{ref}}$  (which is the least dominant one). In Figs. 29-33 we show some cases in which the initial generated image is not in the middle of the small circle path and therefore in these cases, we need to take a different number of steps to each side. The endpoints are defined as the points where the cosine in Eq. 11 becomes 0 and 1.

We do not have to choose the reference direction  $v_{\text{ref}}$  to be the least dominant one. If we choose it to be a dominant direction, then we may obtain various interesting phenomena, depending on the interaction between the directions  $v$  and  $v_{\text{ref}}$ . This is illustrated in Figs. 37-39. Specifically, in Fig. 37 and 38, we perform a walk in the direction corresponding to zoom, while allowing only the vertical shift to change. In this case, the walk manages to center the object so as to achieve a significant zoom effect. In Fig. 39, on the other hand, we perform a walk in the direction corresponding to zoom while allowing only the rotation to change. Here, the zoom effect is less dominant, but we do see a strong rotation effect.

### A.2.3 SECOND ORDER DATASET BIASES

In Figs. 40 and 41 we show more examples for second order dataset biases. Specifically, those figures depict the joint distributions of area and horizontal center shift (top) and area and vertical center shift (bottom) at the end of walks that are supposed to induce only zoom-in. Our small circle walks exhibit the smallest undesired shifts.

### A.2.4 COMPARISONS WITH GANSPACE

In Fig. 42-46, we show visual comparisons with GANSpace (Härkönen et al., 2020). We specifically focus on the first 50 directions founded by each method and show that our linear directions lead to stronger effects for most of the directions. All directions were scaled to have a unit norm and are linearly added or subtracted from the initial latent code with the same step size. In Fig. 48, we show that our direction are orthogonal to each other much more then the directions found by (Härkönen et al., 2020).

## A.3 USER PRESCRIBED SPATIAL MANIPULATIONS

We provide additional examples for walks corresponding to user prescribed geometric transformations. We focus on zoom, vertical shift and horizontal shift, and show both linear and our nonlinear trajectories.

### A.3.1 COMPARISONS WITH JAHANIAN ET AL.

In Figs. 49 we show additional comparisons with Jahanian et al. (2020).

### A.3.2 ADDITIONAL RESULTS

In Figs. 50-53 we show additional zoom trajectories and and in Fig. 54, 55 additional shift trajectories. As can be seen, the linear trajectories often remain more loyal to the original image (at the center) after a small number of steps. However, for a large number of steps, the nonlinear trajectories lead to more plausible images.

---

### A.3.3 RESULTS ON DCGAN

In Figs. 56 - 58, we show results with ResNet based GAN presented in Miyato et al. (2018). That GAN has a FC layer as the first stage, which is all we need in order to perform our spatial manipulations and to extract principal components. Since that architecture is not an hierarchical one, we can manipulate the first layer only.

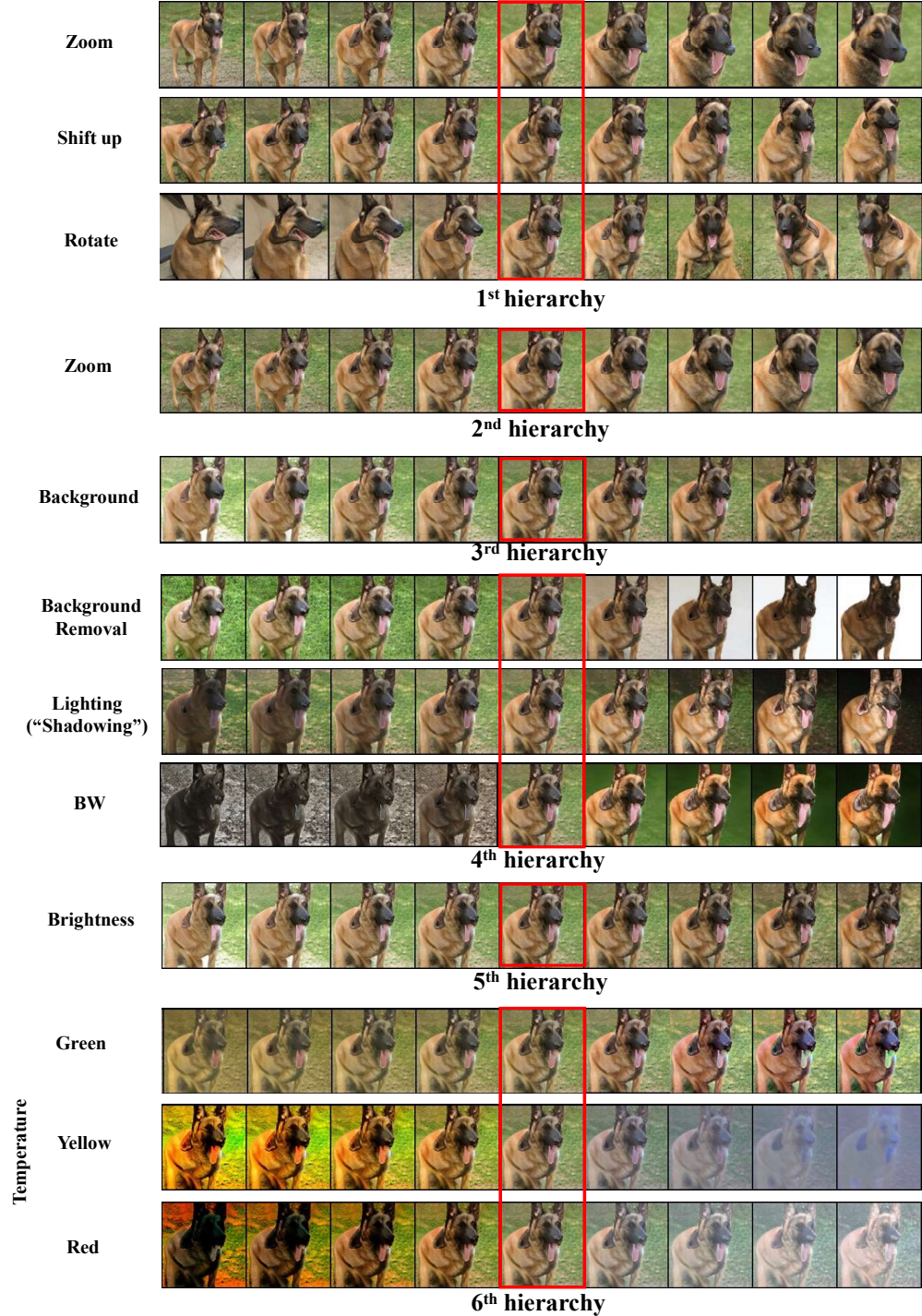


Figure 9: Our explored directions in BigGAN.

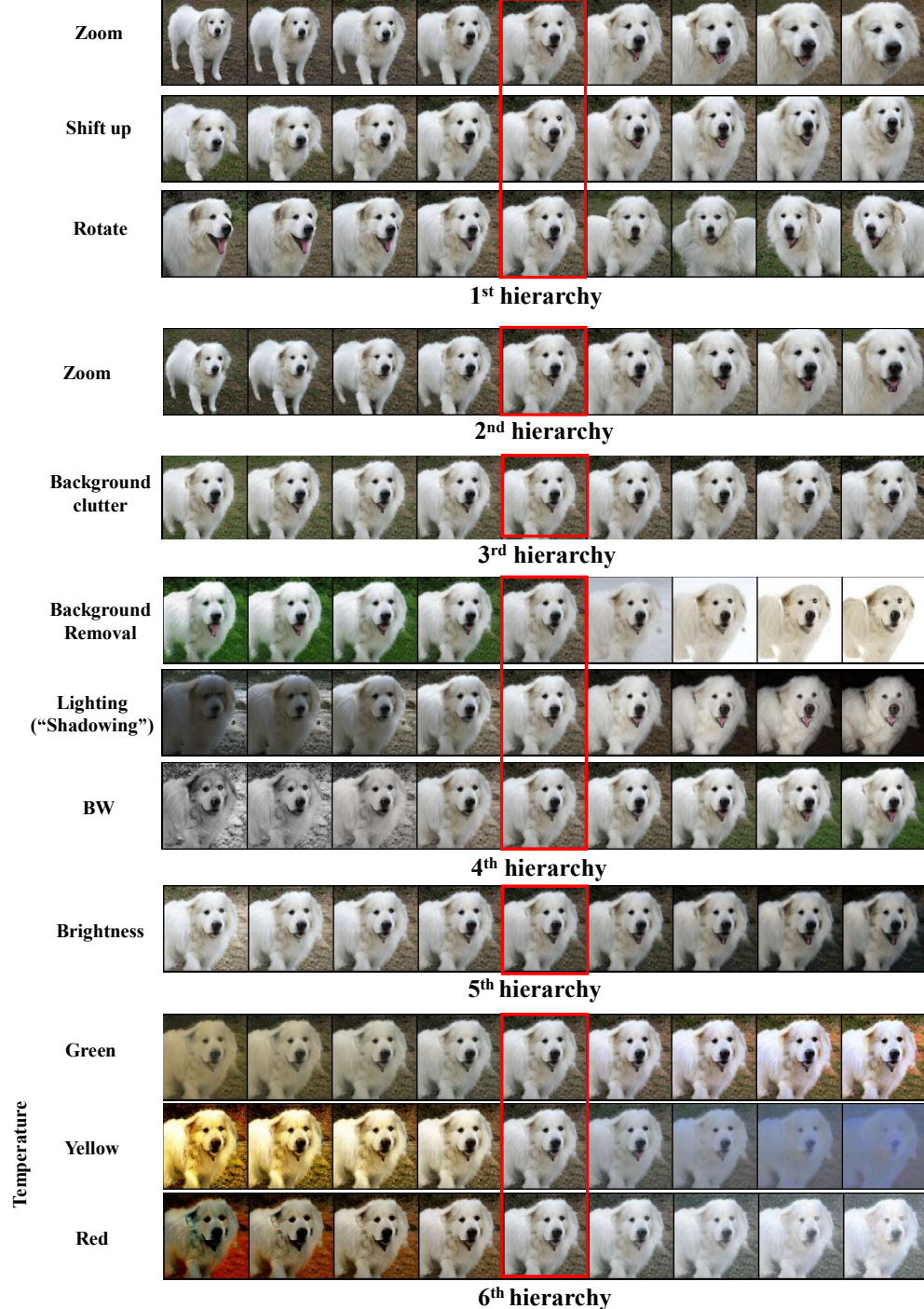


Figure 10: Our explored directions in BigGAN.

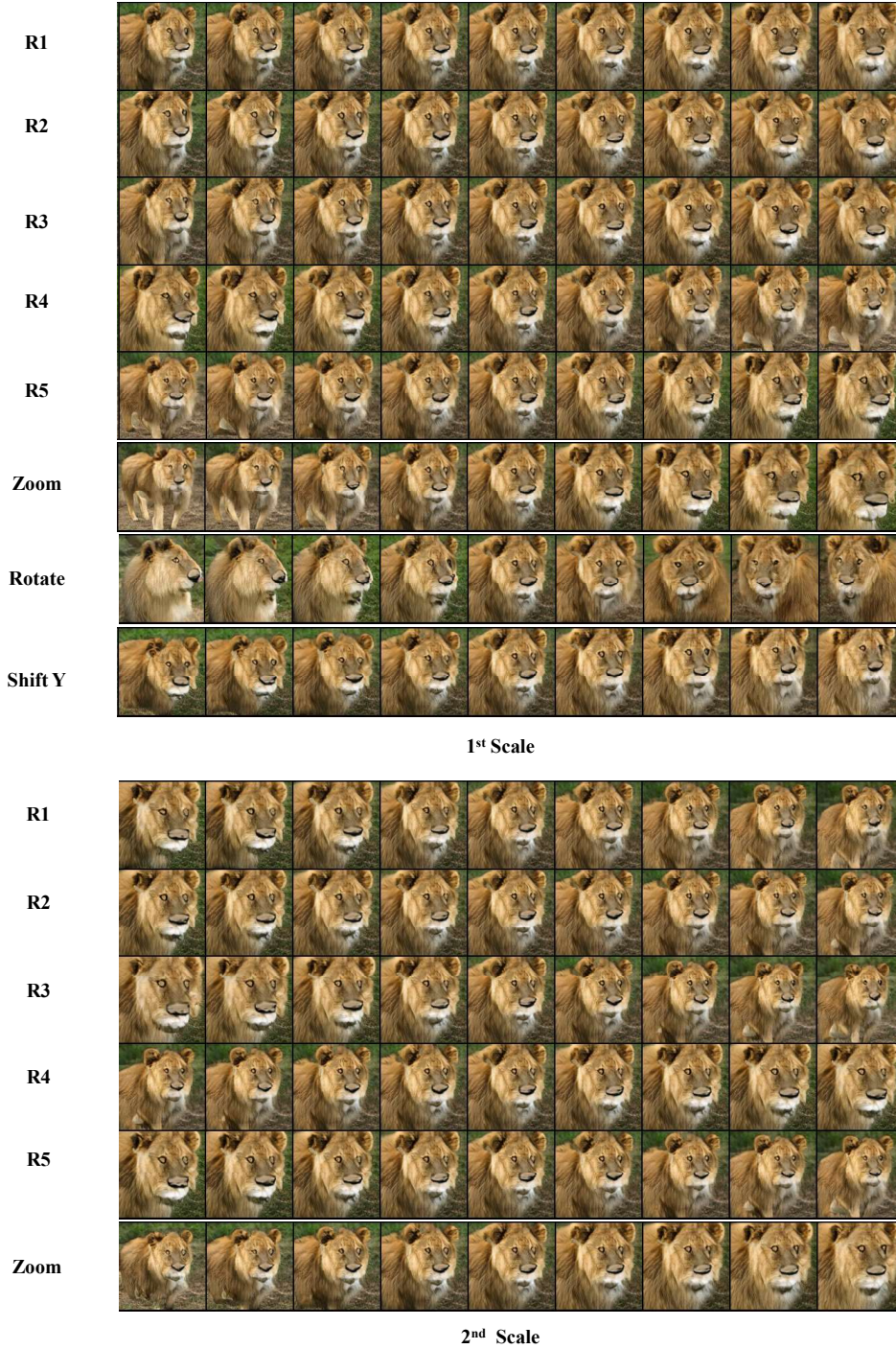


Figure 11: **Our vs. random directions.** We illustrate the effects of five random directions  $R_1, \dots, R_5$  (normally distributed and scaled to have unit norms) in the first and second scales of BigGAN, in comparison with our principal directions. We can see that each random direction leads to different changes, but it is impossible to associate a single dominant property with each direction. For example, in  $R_5$  we can see changes in size, location, and pose. This is while our directions separate those effects into unique paths.

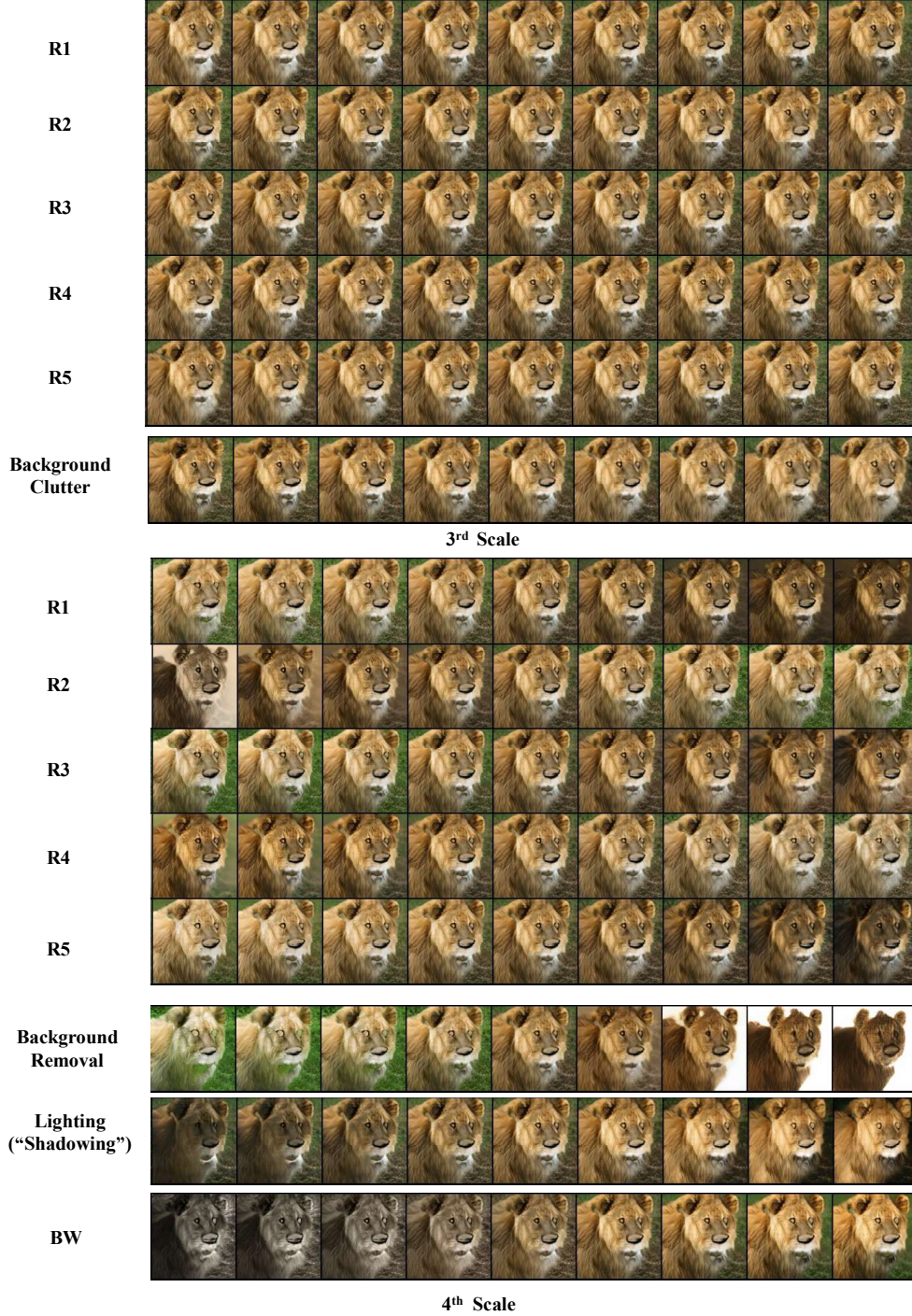


Figure 12: **Our vs. random directions.** We show the effects of five random directions in the third and fourth scales of BigGAN in comparison with our principal directions.

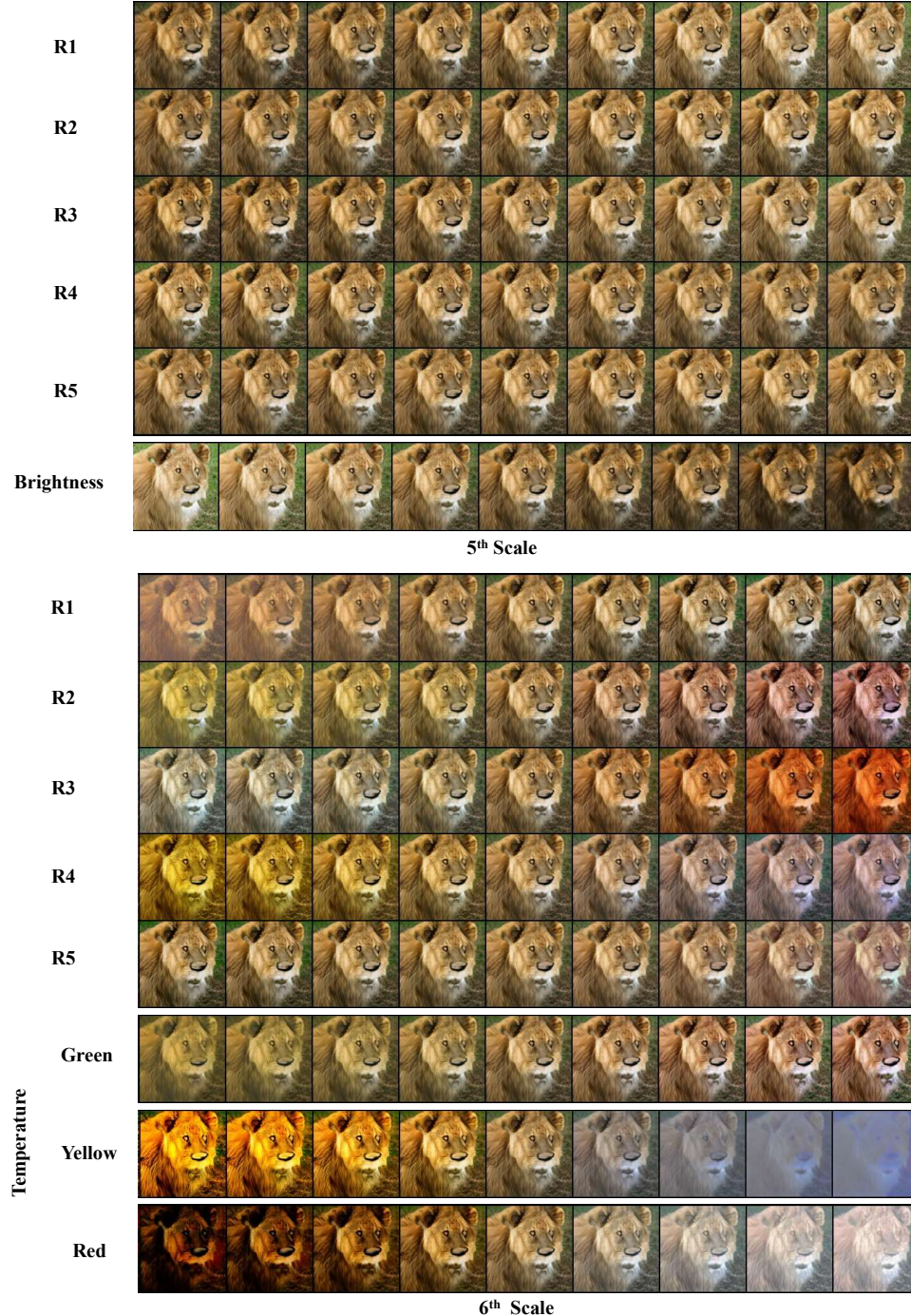


Figure 13: **Our vs. random directions.** We show the effects of five random directions in the fifth and sixth scales of BigGAN in comparison with our principal directions.

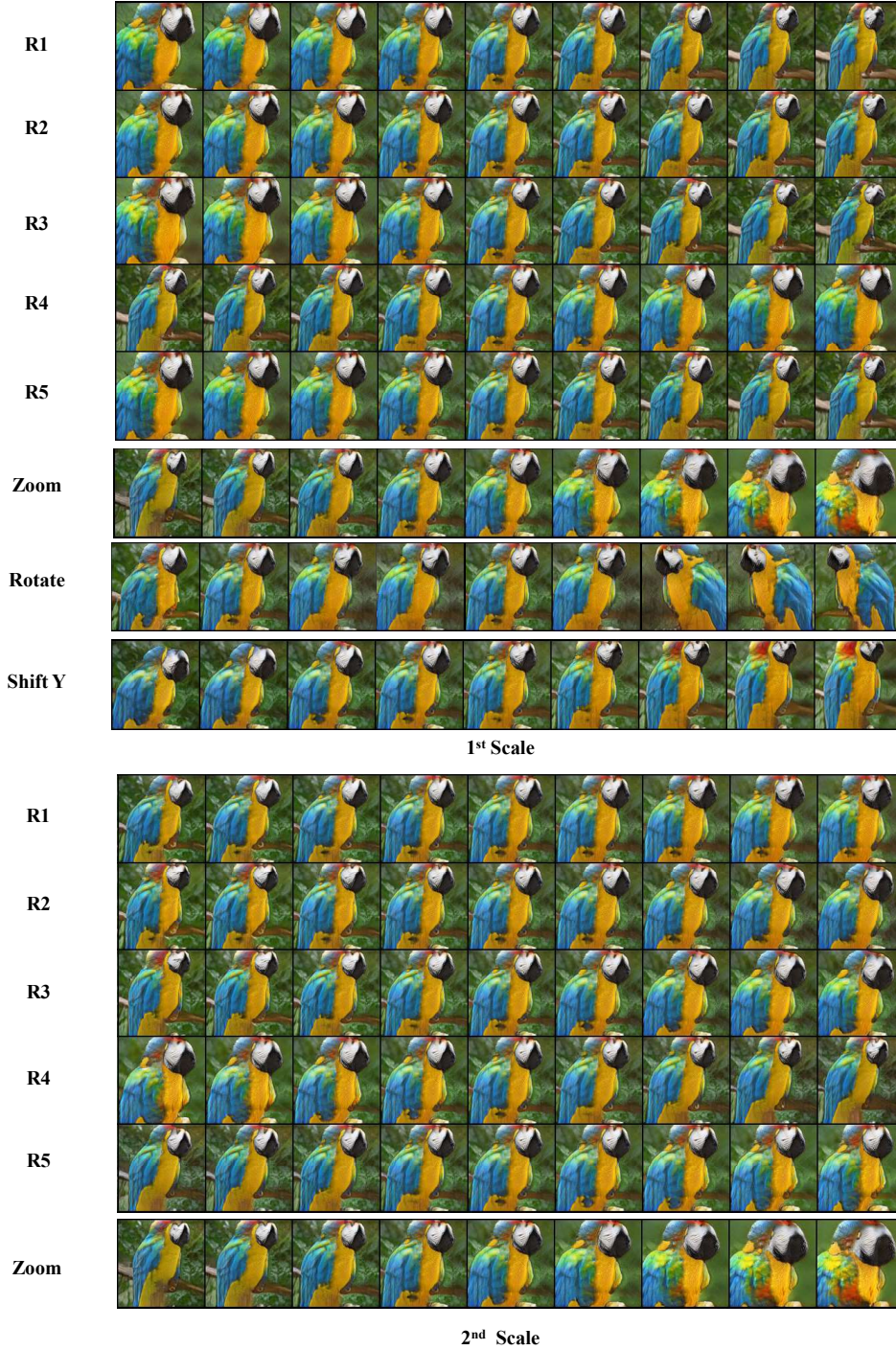


Figure 14: **Our vs. random directions.** We illustrate the effects of five random directions  $R_1, \dots, R_5$  (normally distributed and scaled to have unit norms) in the first and second scales of BigGAN, in comparison with our principal directions. We can see that each random direction leads to different changes, but it is impossible to associate a single dominant property with each direction. For example, in  $R_5$  we can see changes in size, location, and pose. This is while our directions separate those effects into unique paths.

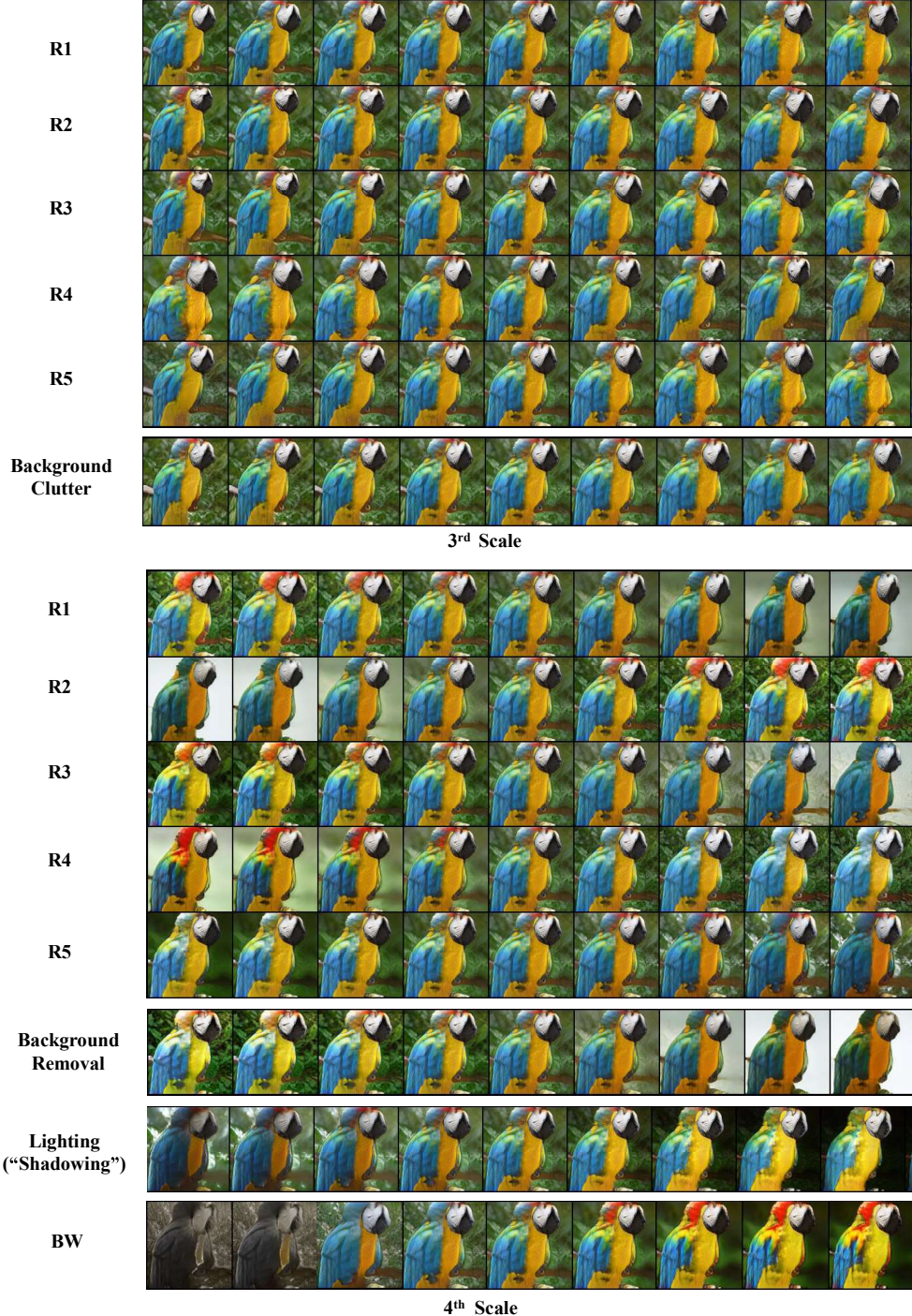


Figure 15: **Our vs. random directions.** We show the effects of five random directions in the third and fourth scales of BigGAN in comparison with our principal directions.

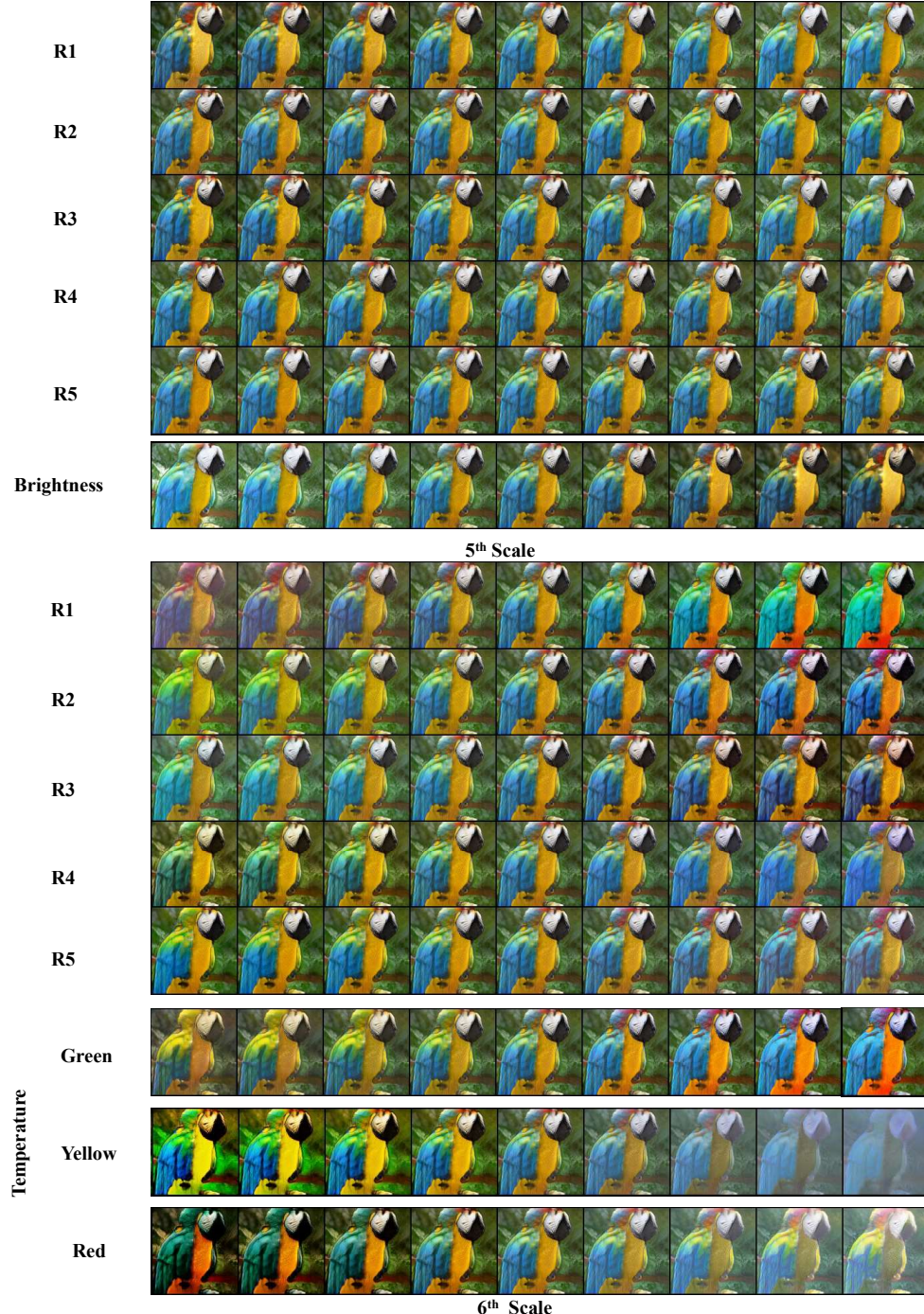


Figure 16: **Our vs. random directions.** We show the effects of five random directions in the fifth and sixth scales of BigGAN in comparison to our principal directions.

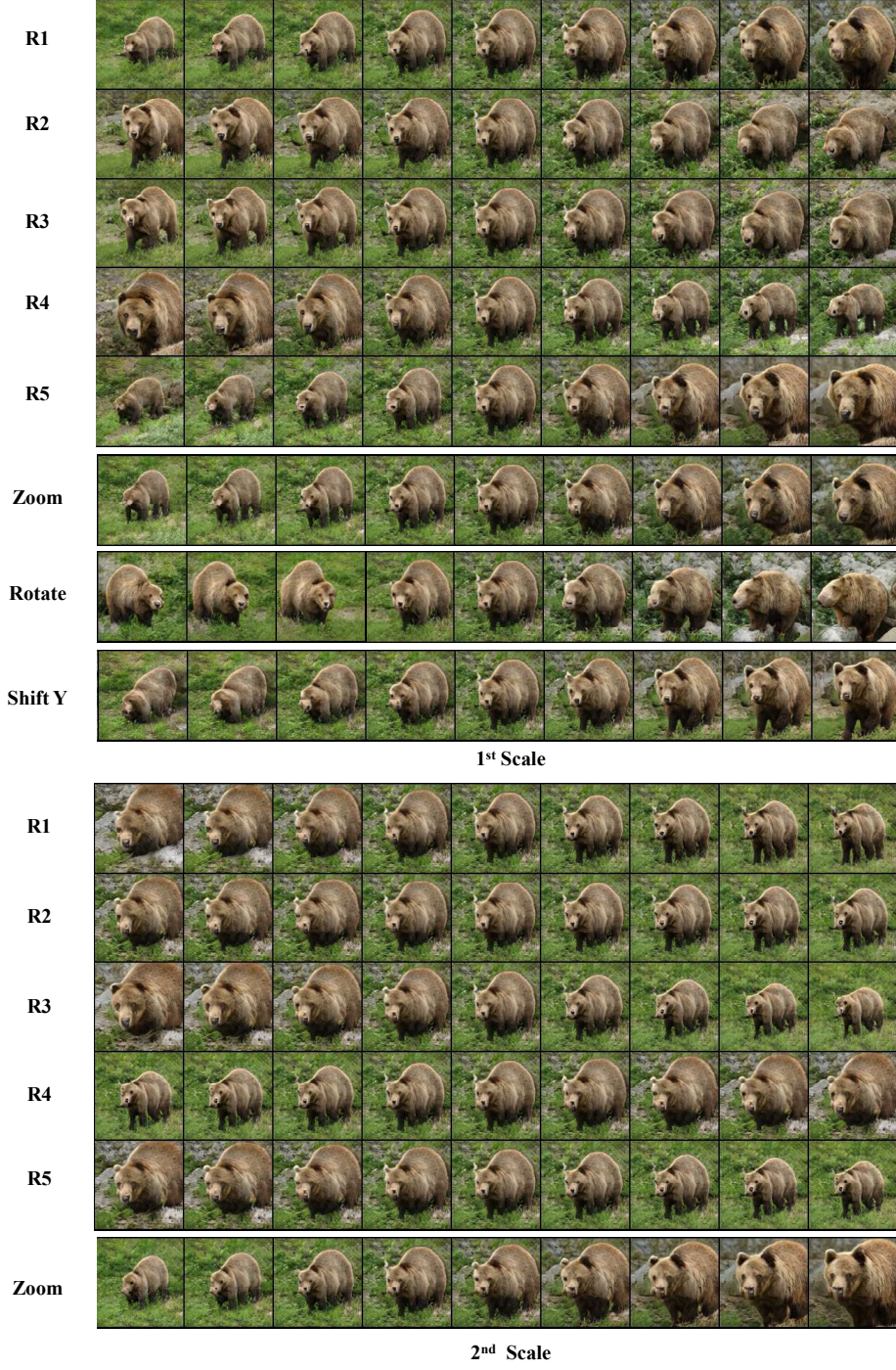


Figure 17: **Our vs. random directions.** We illustrate the effects of five random directions  $R_1, \dots, R_5$  (normally distributed and scaled to have unit norms) in the first and second scales of BigGAN, in comparison with our principal directions. We can see that each random direction leads to different changes, but it is impossible to associate a single dominant property with each direction. For example, in  $R_5$  we can see changes in size, location, and pose. This is while our directions separate those effects into unique paths.

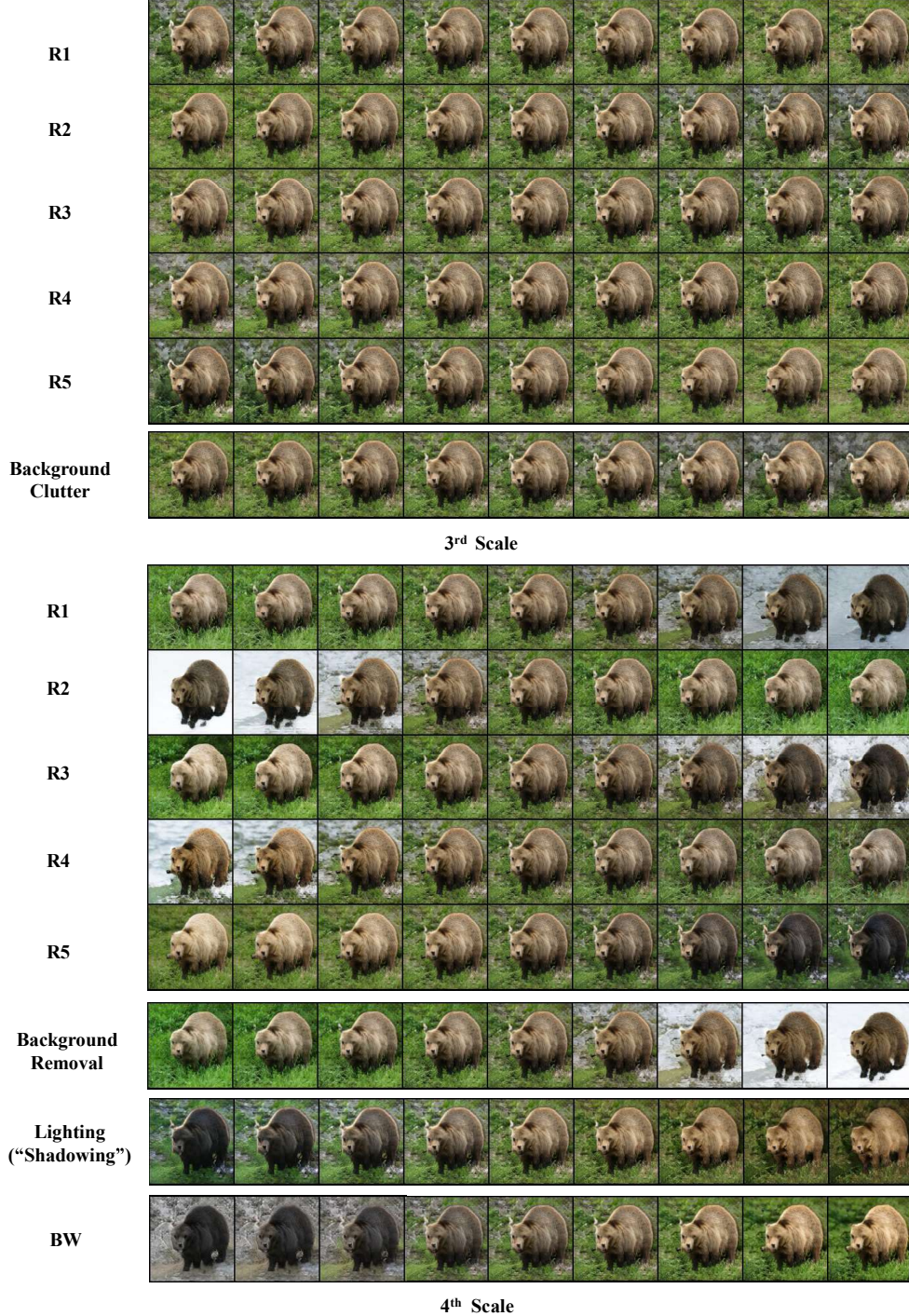


Figure 18: **Our vs. random directions.** We show the effects of five random directions in the third and fourth scales of BigGAN in comparison with our principal directions.

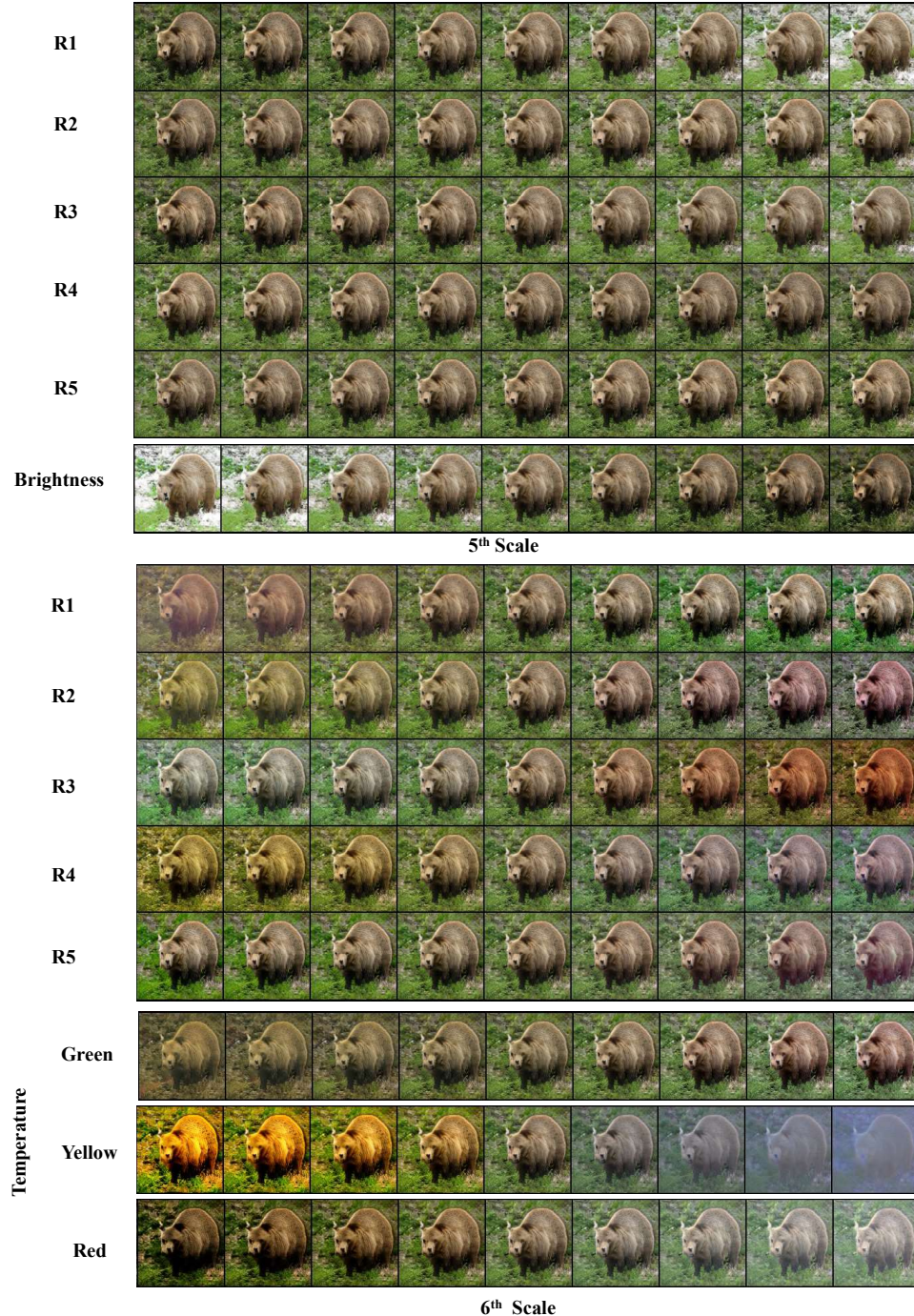


Figure 19: **Our vs. random directions.** We show the effects of five random directions in the fifth and sixth scales of BigGAN in comparison to our principal directions.

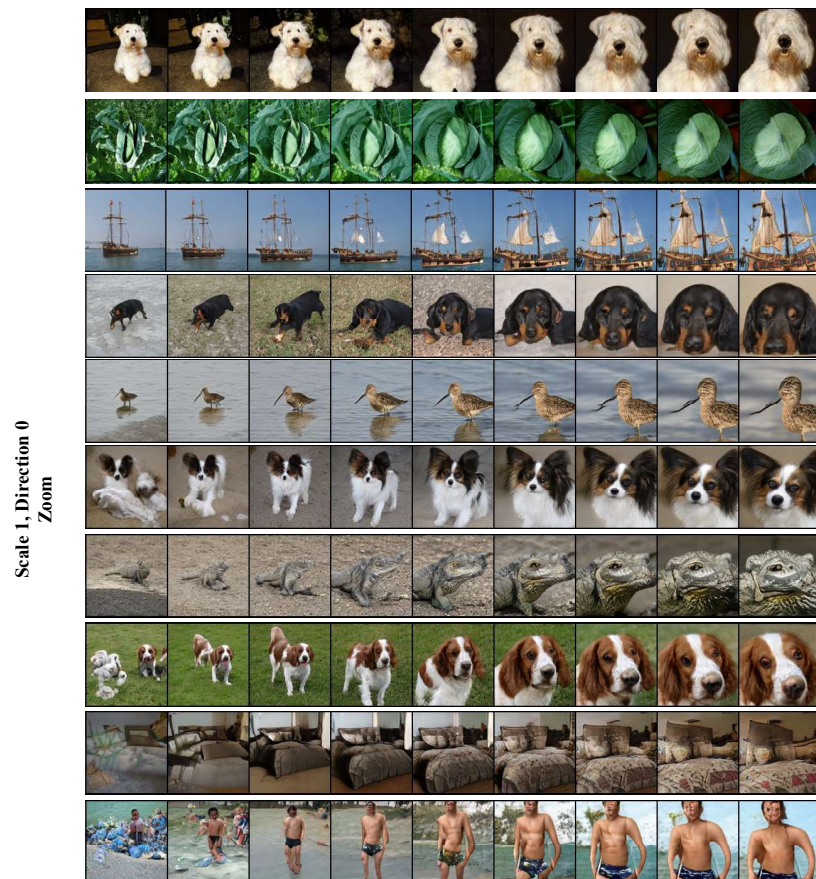


Figure 20: 1st principal direction of the first scale in BigGAN

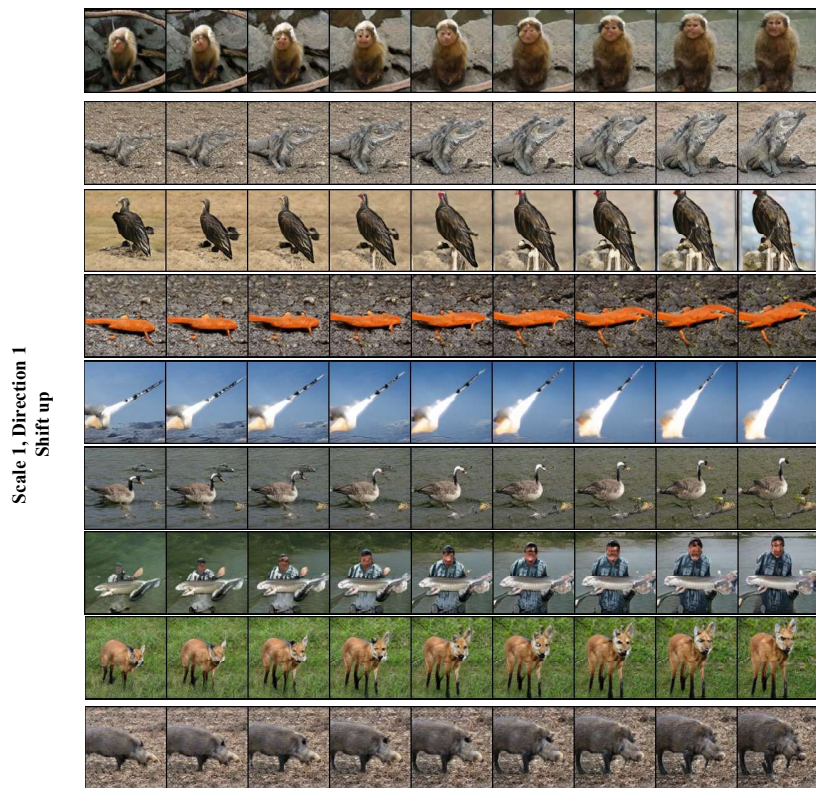


Figure 21: 2nd principal direction of the first scale in BigGAN

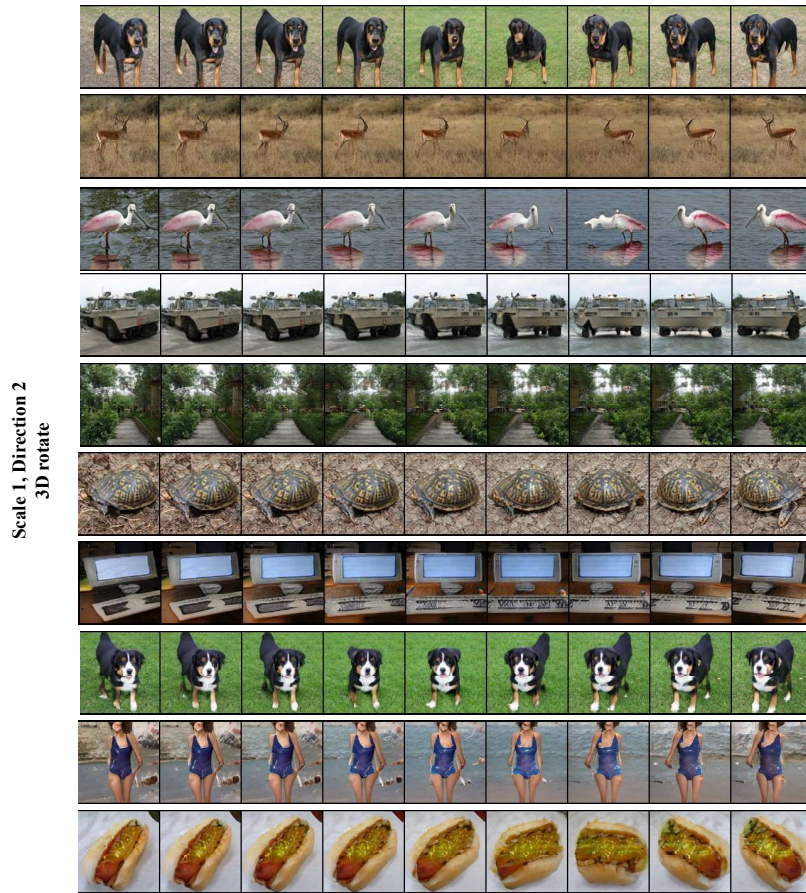


Figure 22: 3rd principal direction of the first scale in BigGAN

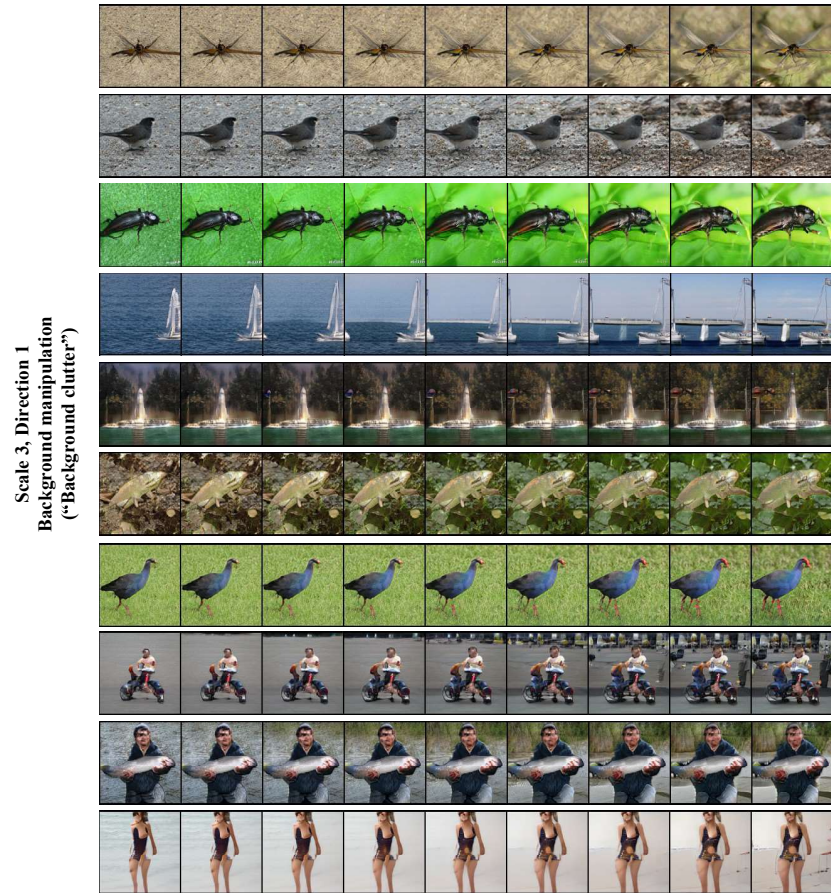


Figure 23: 1st principal direction of the third scale in BigGAN

Scale 4, Direction 1  
Background Removal

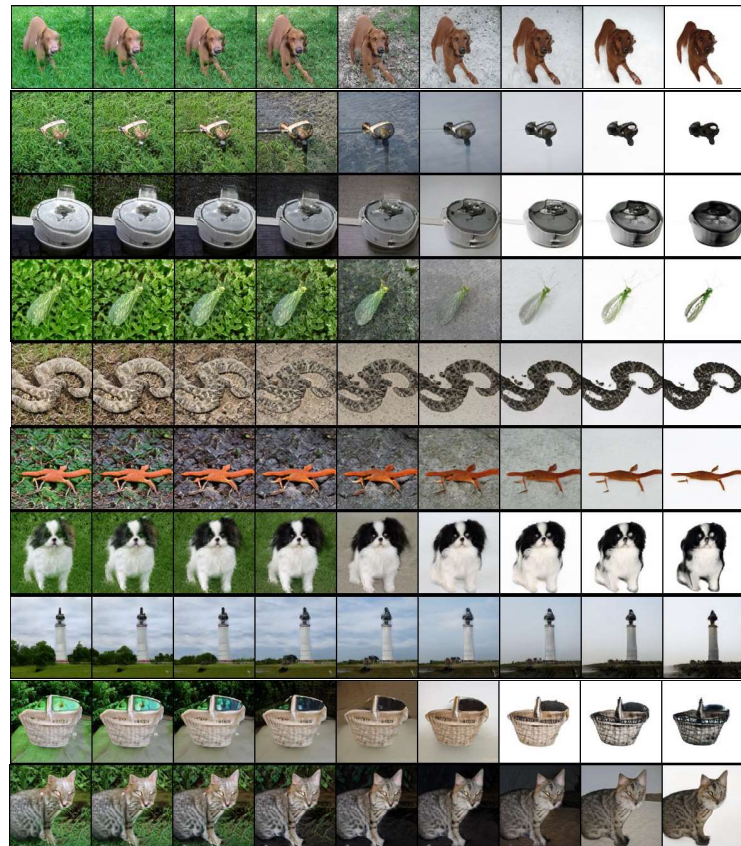


Figure 24: First principal direction of the fourth scale in BigGAN

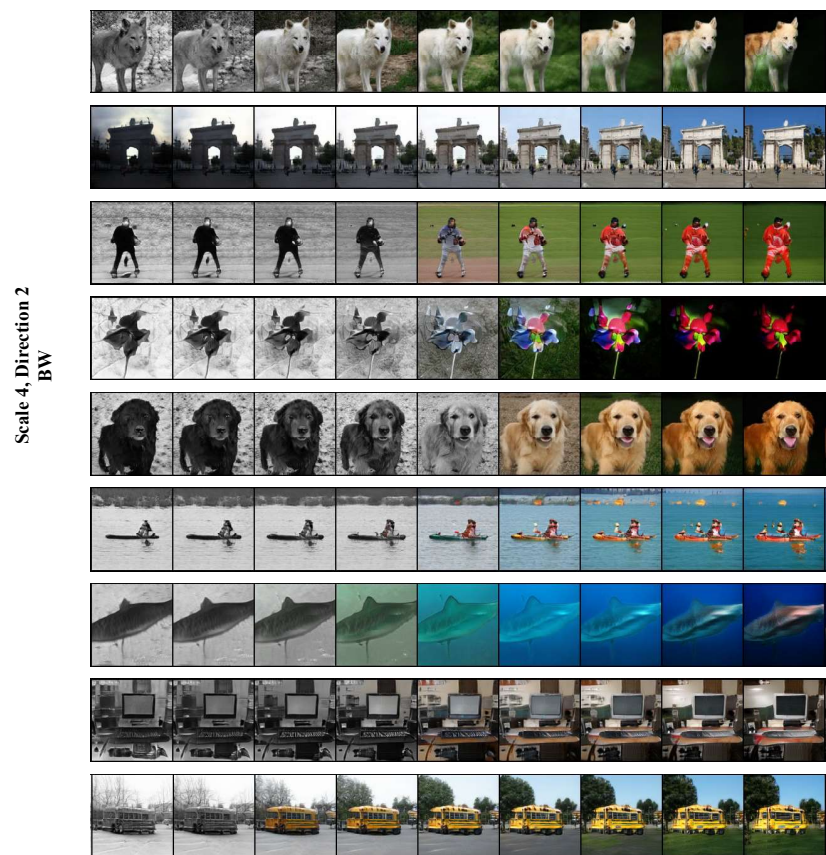


Figure 25: Second principal direction of the fourth scale in BigGAN

Scale 4, Direction 3  
Lighting (“Shadowing”)

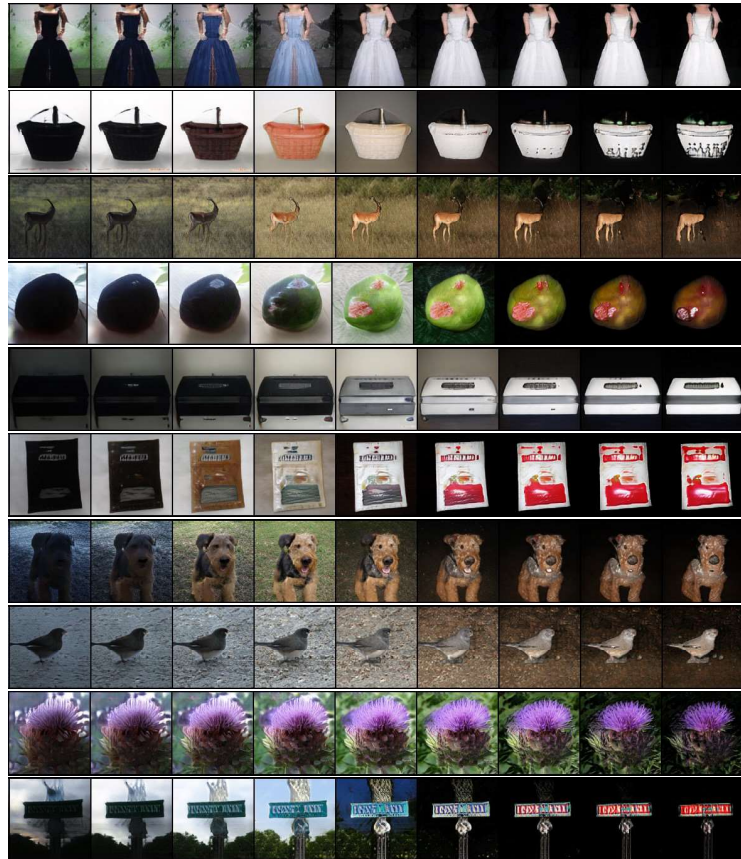


Figure 26: Third principal direction of the fourth scale in BigGAN

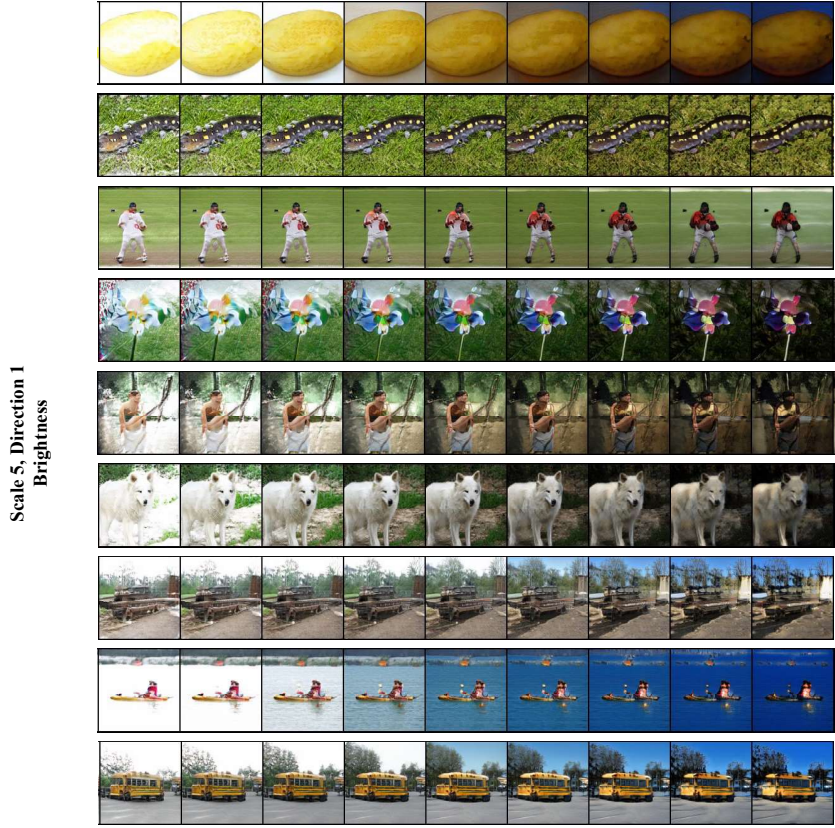


Figure 27: First principal direction of the fifth scale in BigGAN

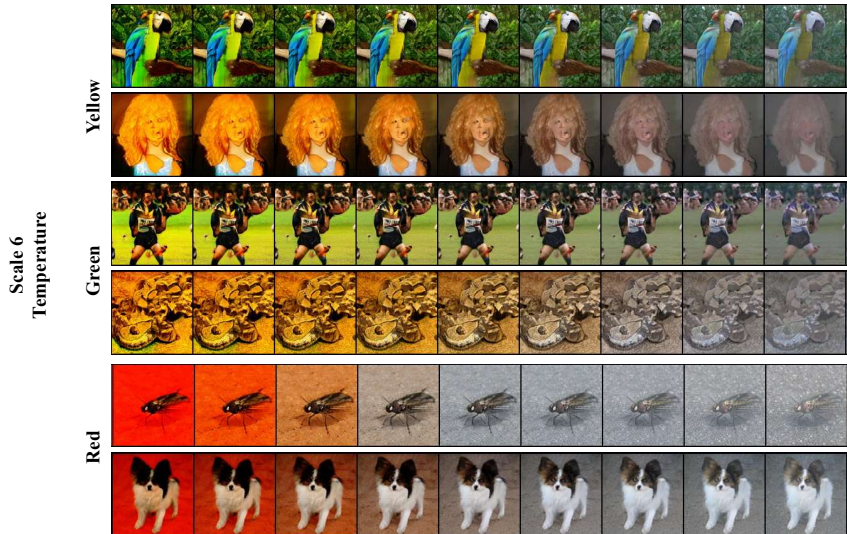


Figure 28: First three principal direction of the sixth scale in BigGAN

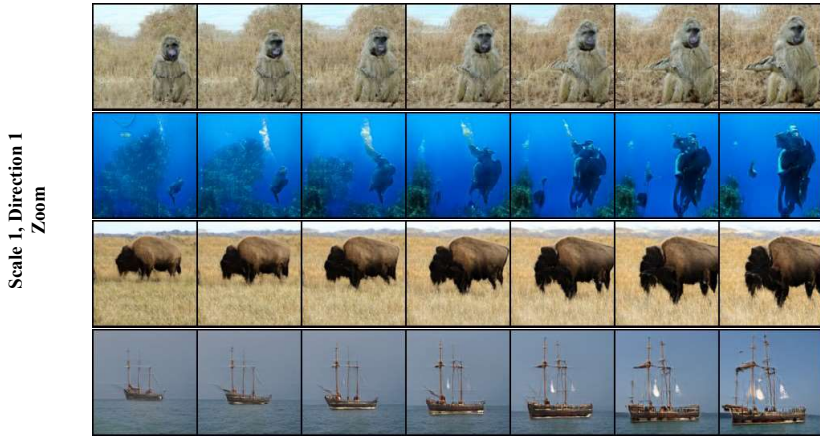


Figure 29: First principal direction of scale 1 in BigGAN (small circle walks).



Figure 30: Second principal direction of scale 1 in BigGAN (small circle walks).

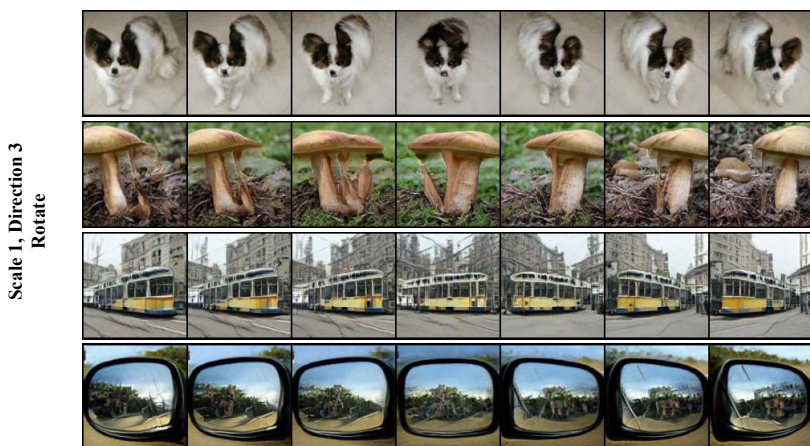


Figure 31: Third principal direction of scale 1 in BigGAN (small circle walks).



Figure 32: Third principal direction of scale 4 in BigGAN (small circle walks).

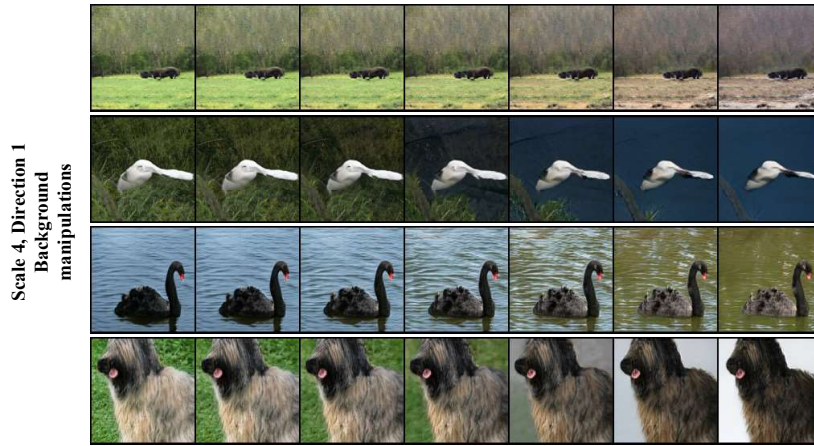


Figure 33: First principal direction of scale 4 (small circle walks). When walking enough steps in the linear direction, a total background removal is observed (see Fig.15. However, it might come with a slight change of object colors. Therefore, we will not constantly see it within the small circle framework (see last image in that bulk in comparison to the other 3).



Figure 34: Second principal direction of scale 4 in BigGAN (small circle walks).



Figure 35: Chosen principal direction of scale 3 in BigGAN (small circle walks). When the initial generated image is not at the middle of the path, we need to take different number of steps to each side.

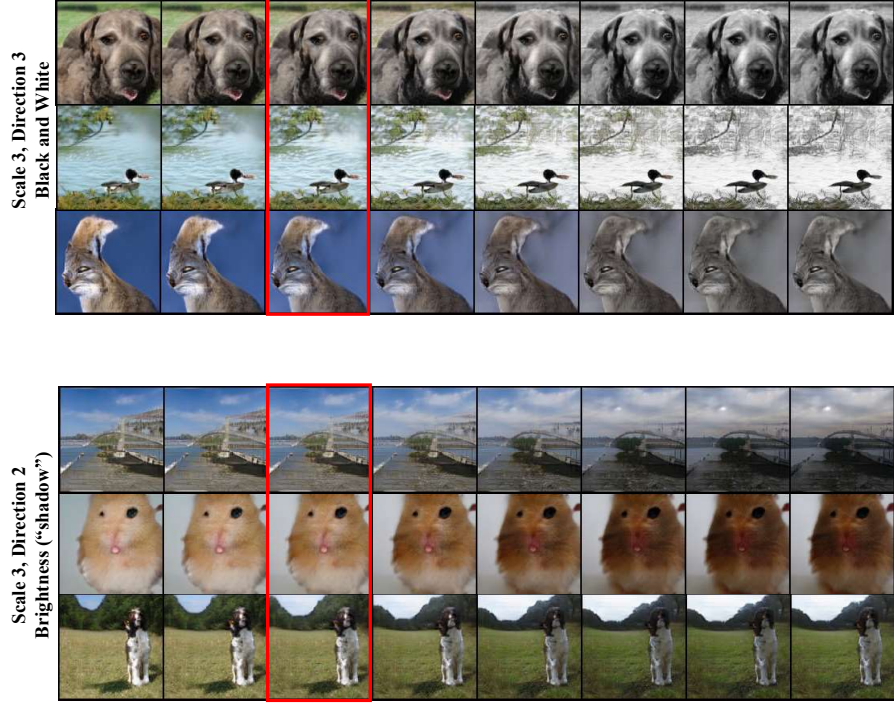


Figure 36: Chosen principal direction of scale 1 in BigGAN (small circle walks). When the initial generated image is not at the middle of the path, we need to take different number of steps at each side.

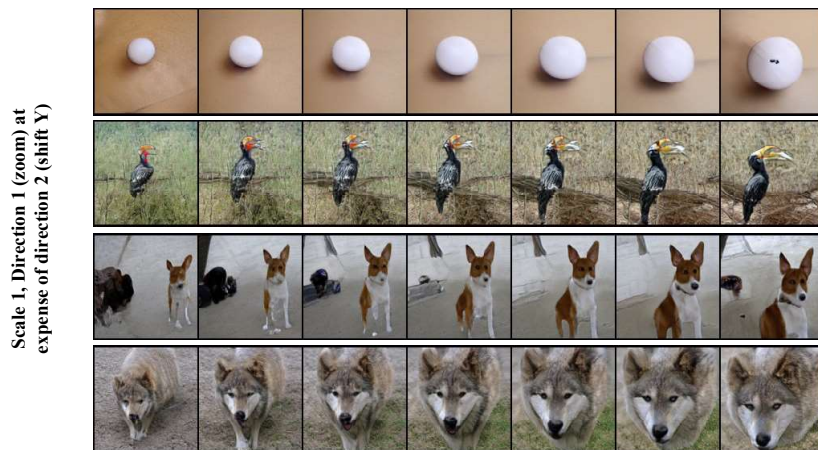


Figure 37: Modifying the second principal direction of scale 1 on the expense of the first principal direction of that scale in BigGAN (small circle walks).

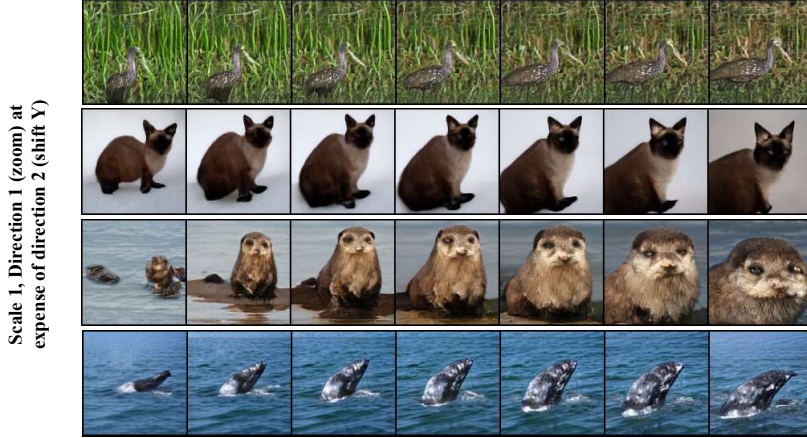


Figure 38: Modifying the second principal direction of scale 1 on the expense of the first principal direction of that scale in BigGAN (small circle walks).

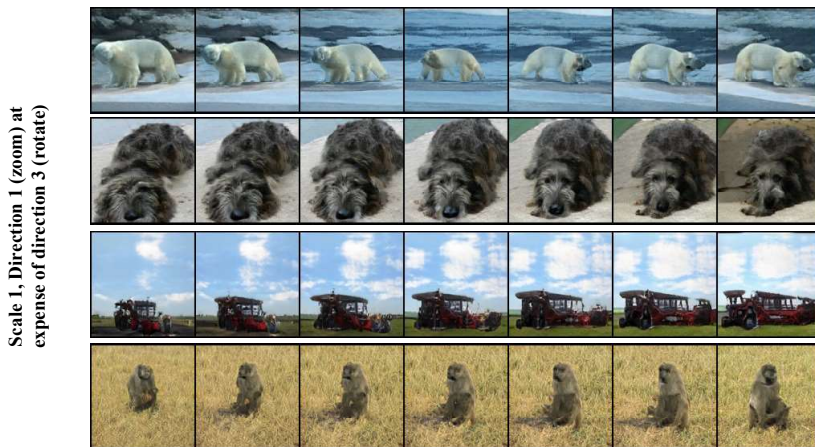
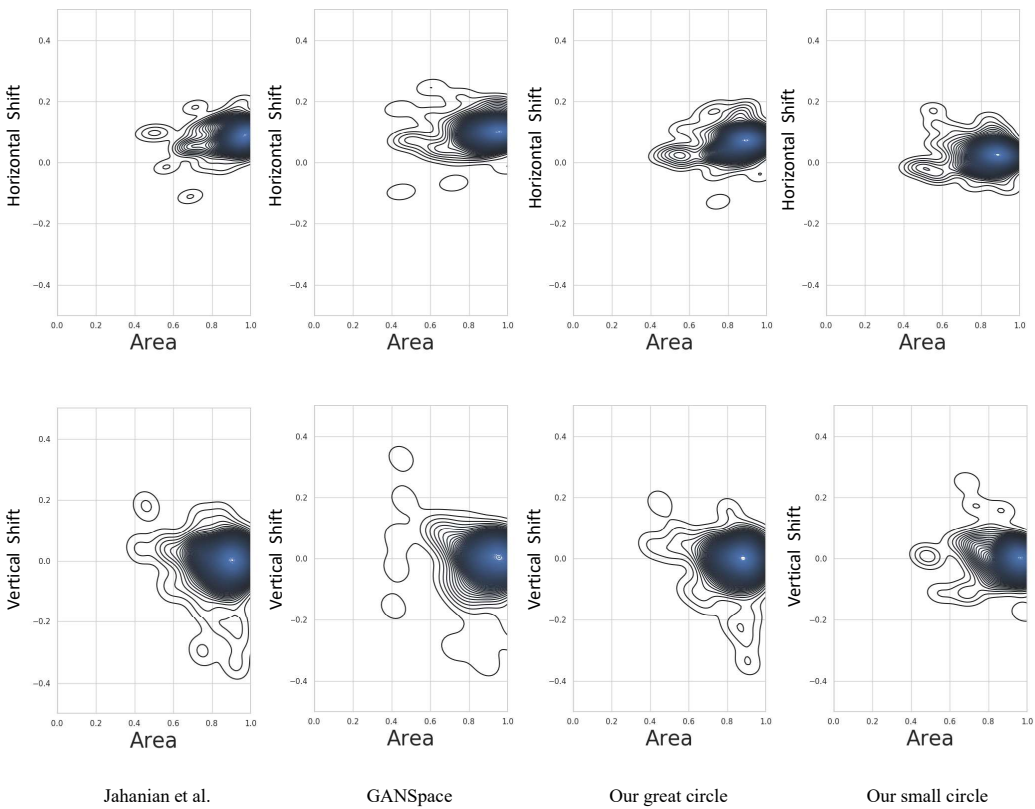
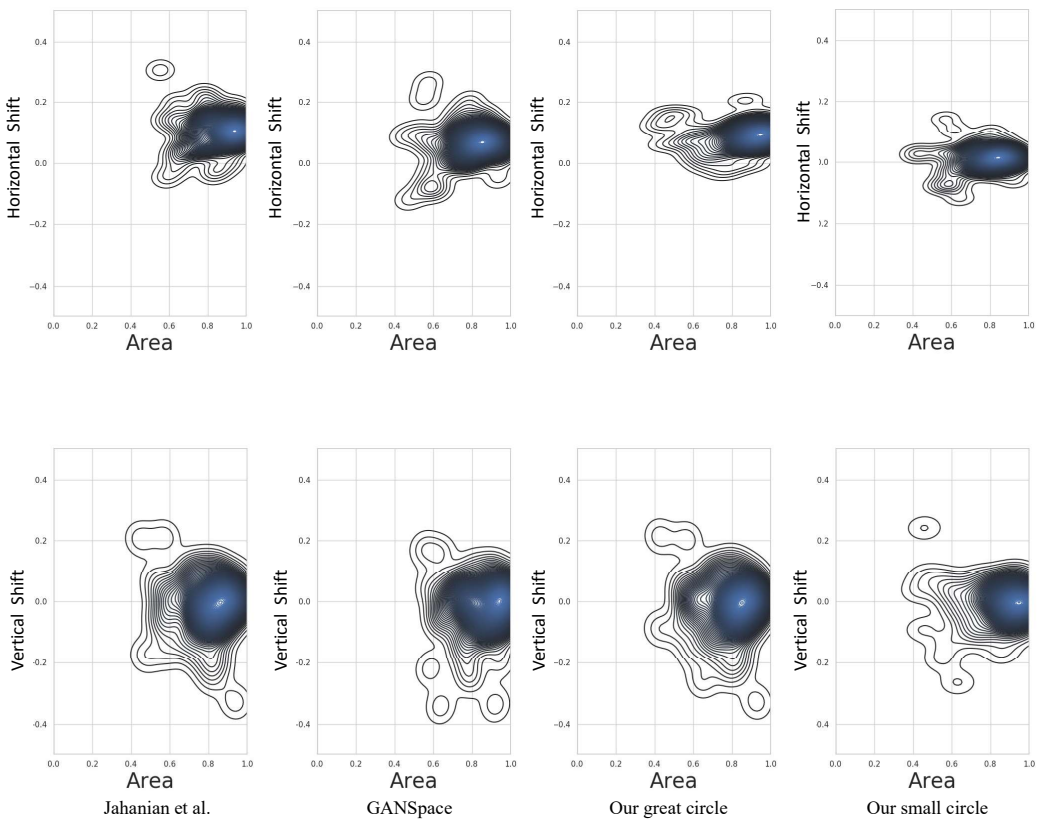


Figure 39: Modifying the third principal direction of scale 1 on the expense of the first principal direction of that scale in BigGAN (small circle walks).



**Figure 40: Second order dataset biases.** We explore the coupling between zoom and horizontal translation (top) and zoom and vertical translation (bottom) for Persian cat class in BigGAN-deep. It can be clearly observed that the small circle path exhibits the smallest undesired shifts when increasing the area.



**Figure 41: Second order dataset biases.** We explore the coupling between zoom and horizontal translation (top) and zoom and vertical translation (bottom) for husky dogs class in BigGAN-deep. It can be clearly observed that the small circle path exhibits the smallest undesired shifts when increasing the area.

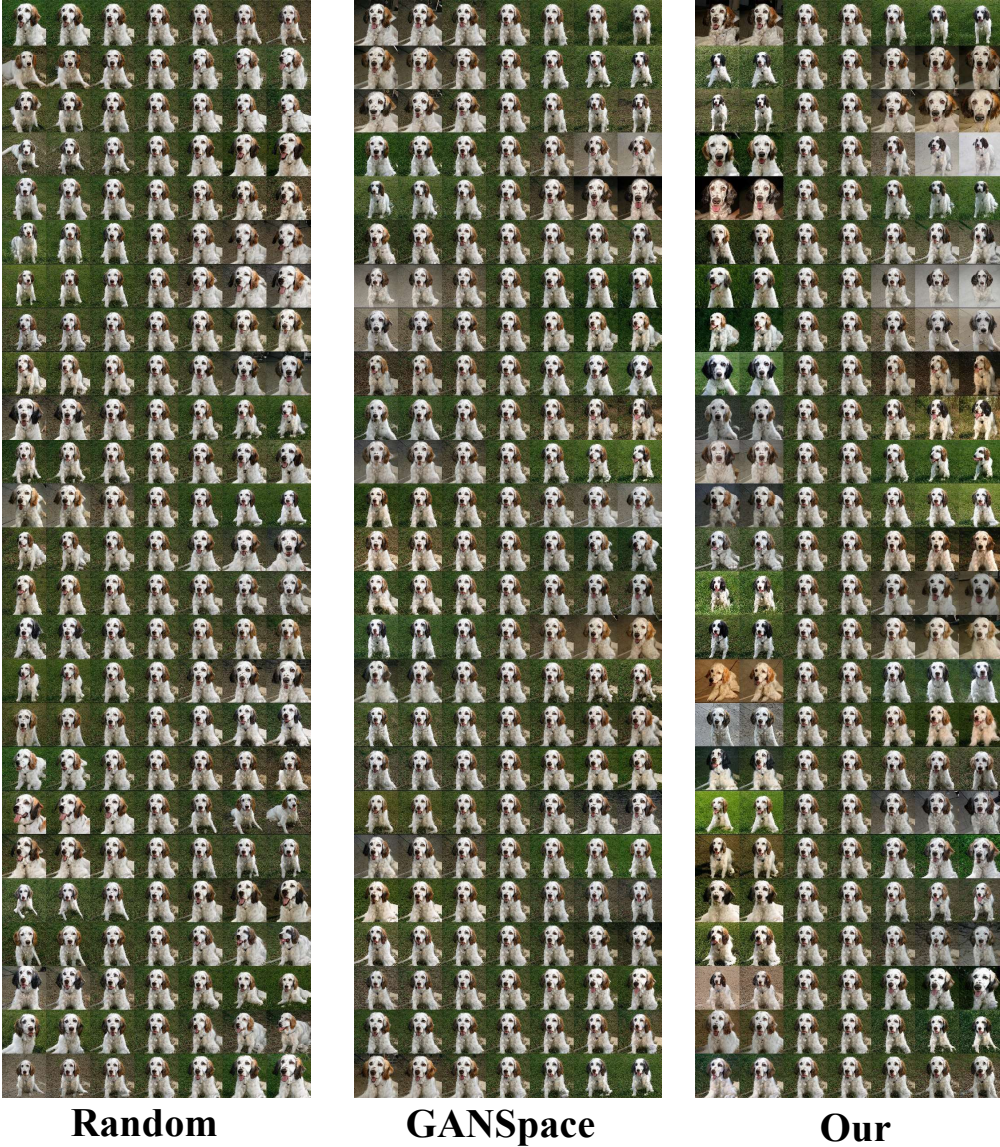


Figure 42: **Comparison with GANSpace and random directions in BigGAN-deep** (principal vectors 0-25). The image at the center of each block is the original image. We linearly added the vectors with equal steps. Both directions are normalized to have unit-norms. We can see that our trajectories induce a stronger change than those of Härkönen et al. (2020). The averaged LPIPS variance is 0.036 and 0.059 for Härkönen et al. (2020) and our method, respectively.

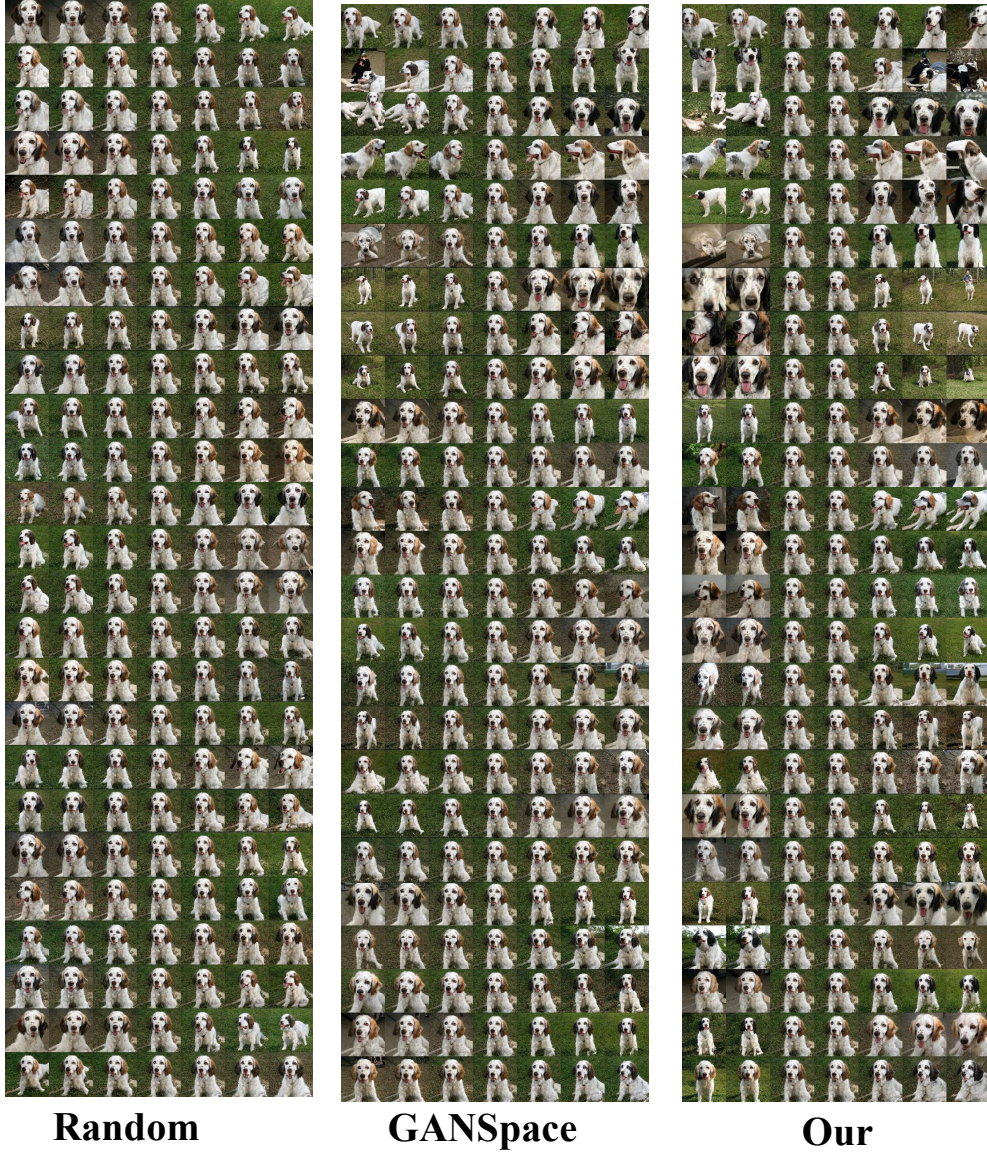


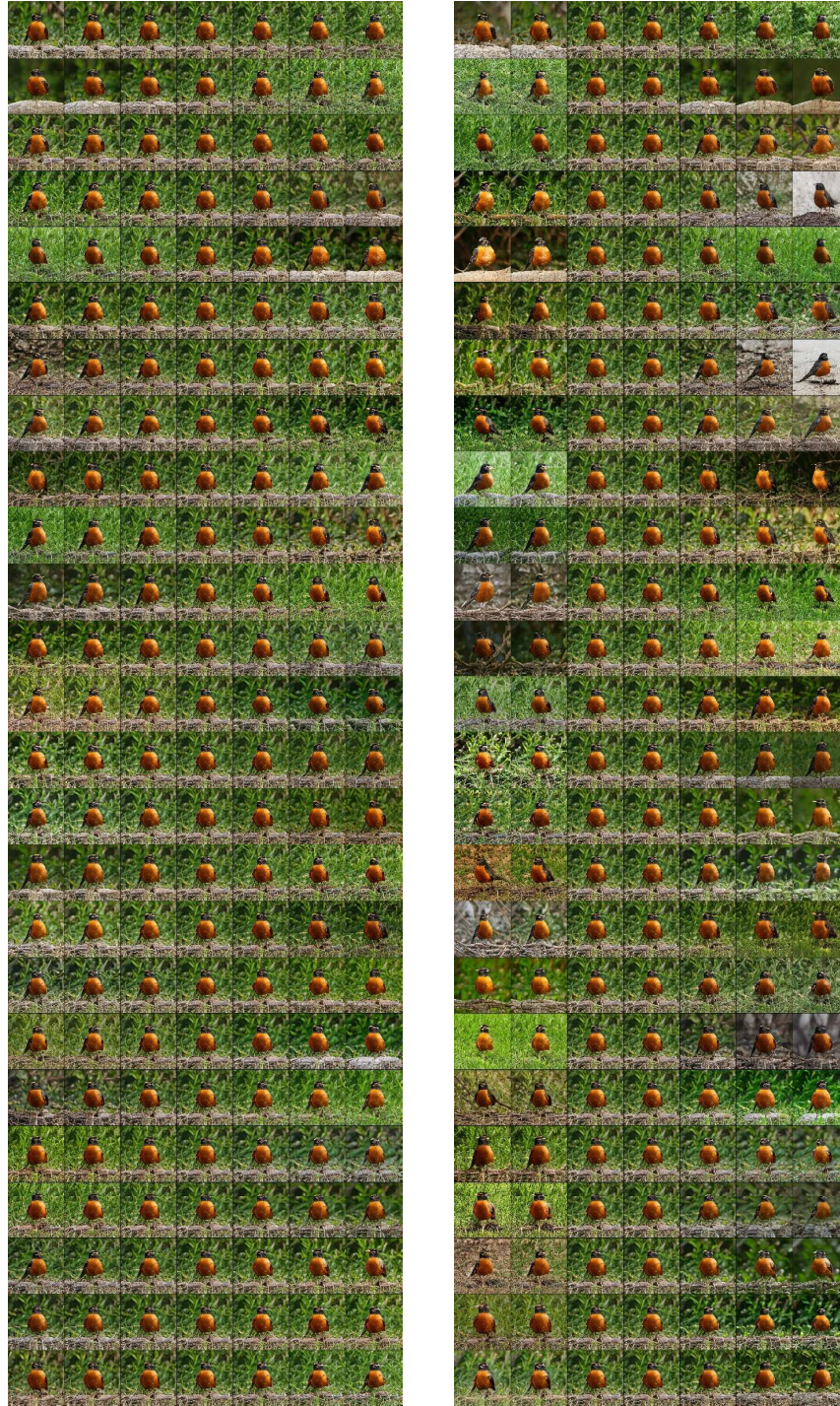
Figure 43: **Comparison with GANSpace and random directions in BigGAN-deep** (principal vectors 25-50). The image at the center of each block is the original image. We linearly added the vectors with equal steps. Both directions are normalized to have unit-norms. It can be observed that our trajectories induce stronger change than those of Härkönen et al. (2020). The averaged LPIPS variance is 0.03 and 0.049 for Härkönen et al. (2020) and our method, respectively.



**GANSpace**

**Our**

Figure 44: **Comparison with GANSpace in BigGAN-deep** (principal directions 0-25). The image at the center of each block is the original image. We linearly added the vectors with equal steps. Both directions are normalized to have unit-norms. It can be observed that our trajectories induce stronger change than those of Härkönen et al. (2020).



**GANSpace**

**Our**

Figure 45: Comparison with GANSpace in BigGAN deep (principal directions 25-50).



**GANSpace**

**Our**

Figure 46: Comparison with GANSpace in bigGAN deep - (principal directions 25-50).

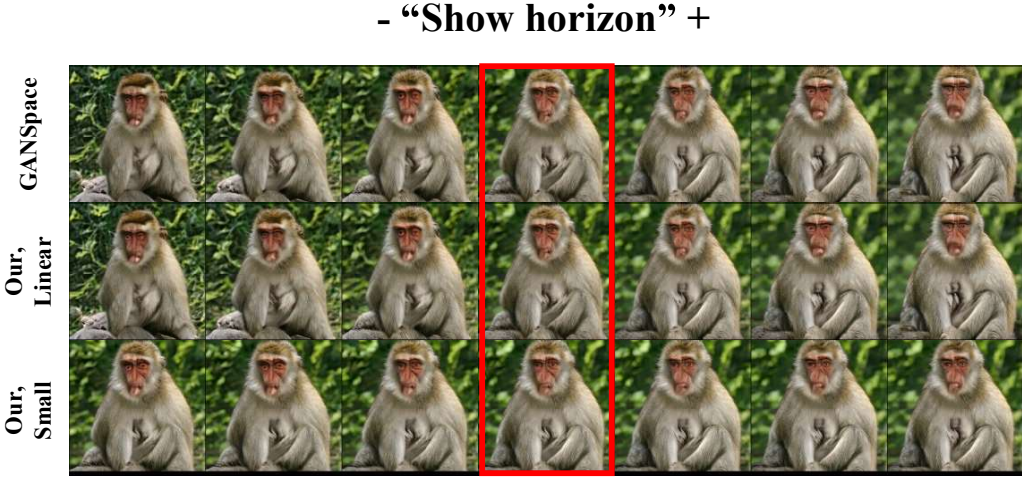


Figure 47: **Comparison with Härkönen et al. (2020)**. An example for the “show horizon” direction which we apply to edit only layers 1-5 (Härkönen et al., 2020) in BigGAN-deep 512. We can see that our linear directions achieve similar effects to those of GANSpace (blurring the background). However, in both cases, we can also see slight changes in the object size and pose. On the other hand, when using our small circle walk, we keep the same size and pose.

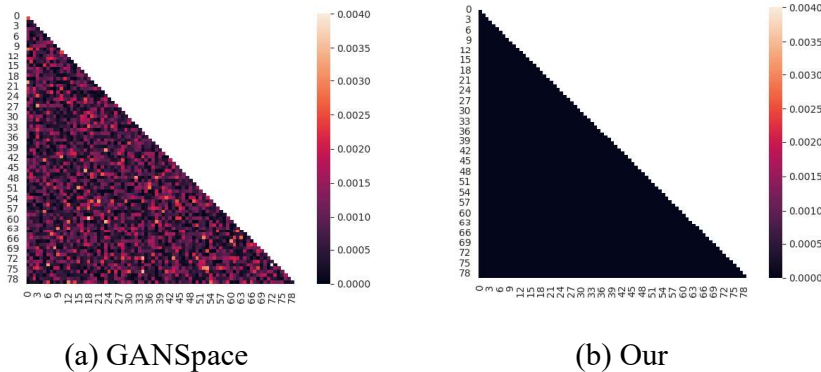


Figure 48: **Evaluating orthogonality**. We show absolute value of the correlation between every two directions among the first 80 directions in GANspace and in our method for BigGAN-deep-512.

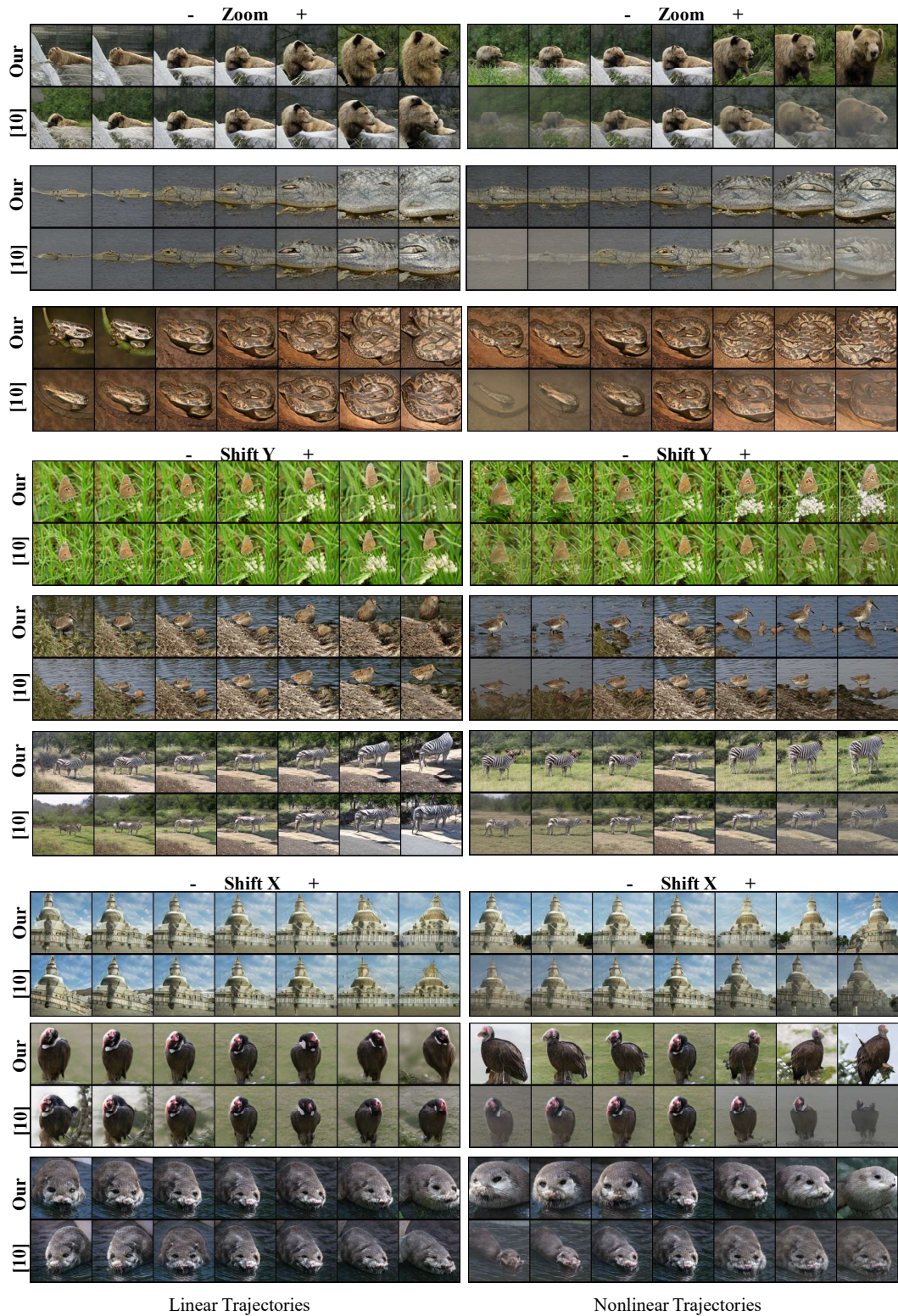


Figure 49: User prescribed transformations with BigGAN.

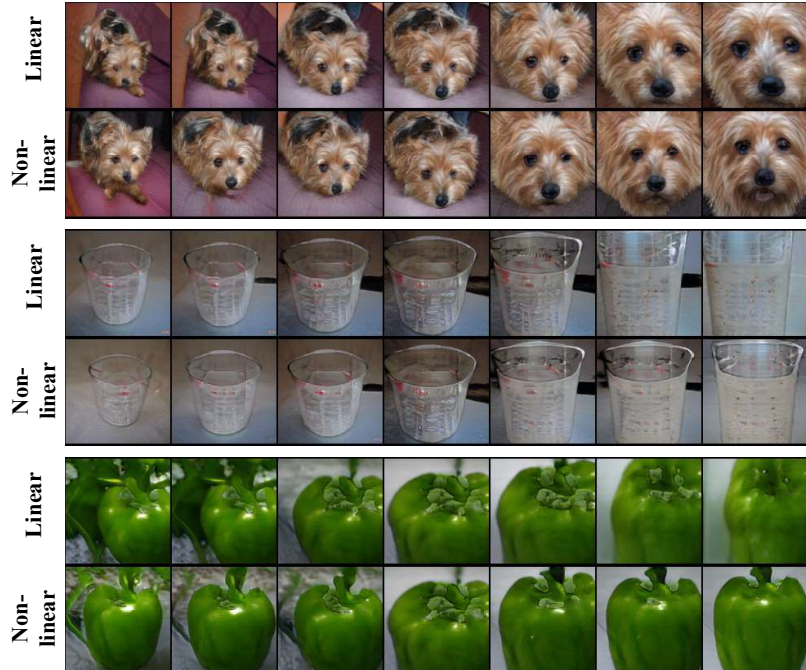


Figure 50: User prescribed zoom with BigGAN. Our method, linear vs. non-linear trajectories.

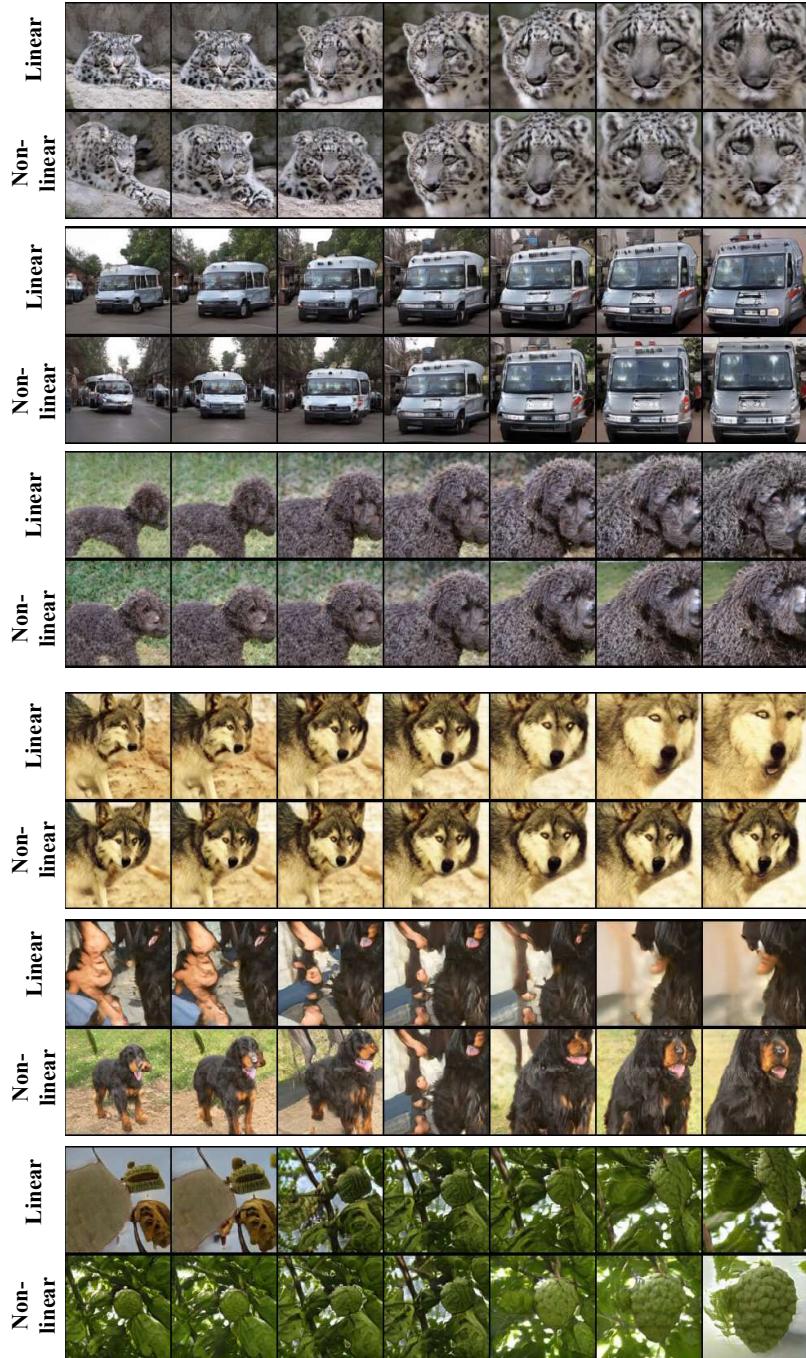


Figure 51: User prescribed zoom with BigGAN. Our method, linear vs non-linear trajectories

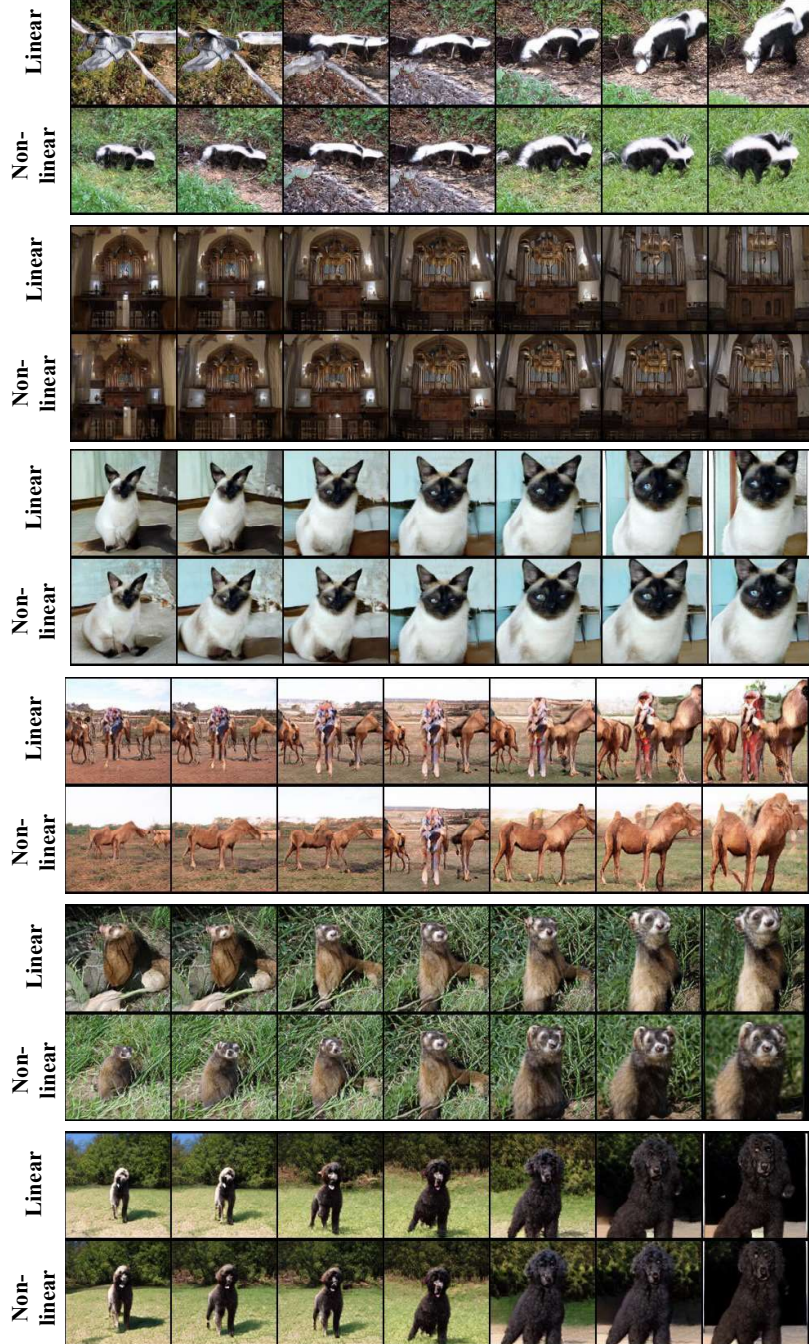


Figure 52: User prescribed zoom with BigGAN . Our method, linear vs. non-linear trajectories.



Figure 53: User prescribed zoom with BigGAN. Our method, linear vs. non-linear trajectories.

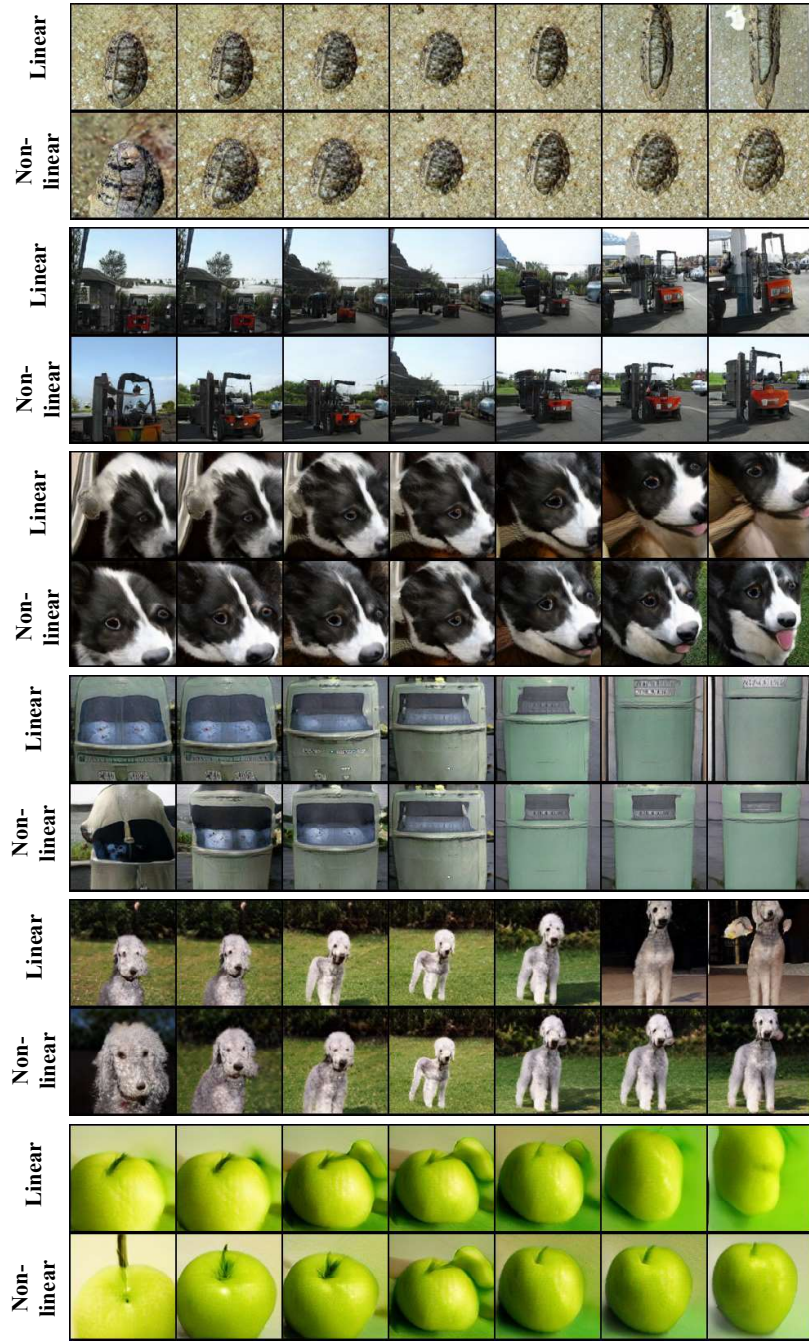


Figure 54: User prescribed vertical shift with BigGAN. Our method, linear vs. non-linear trajectories.

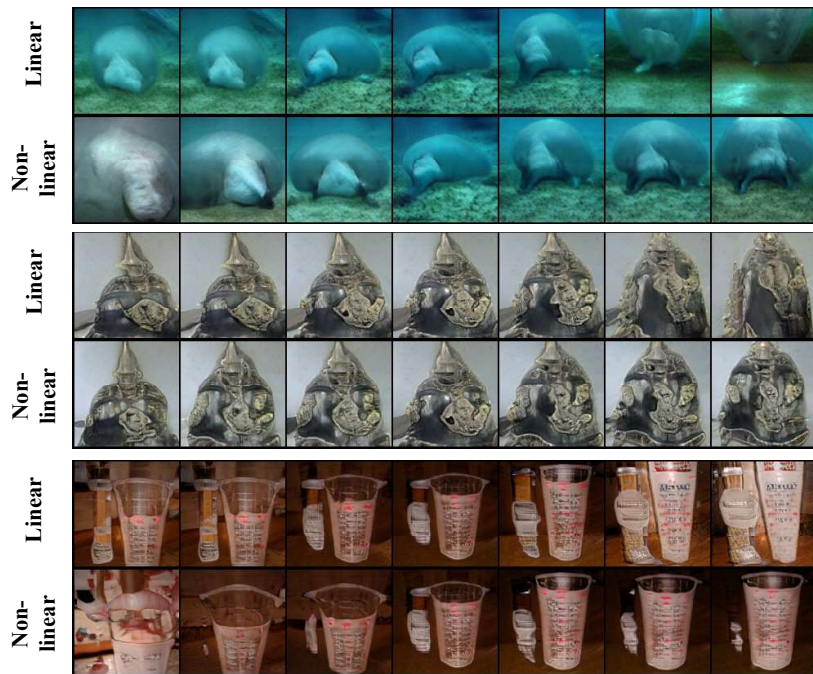


Figure 55: User prescribed vertical shift with BigGAN. Our method, linear vs. non-linear trajectories.

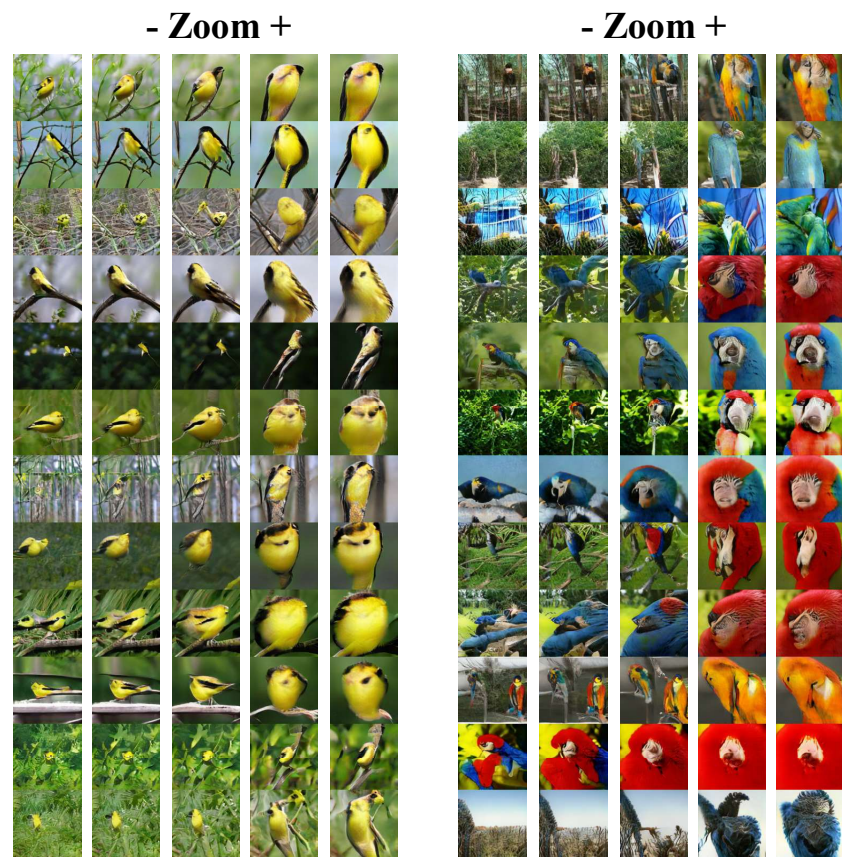


Figure 56: Zoom transformation with DCGAN.

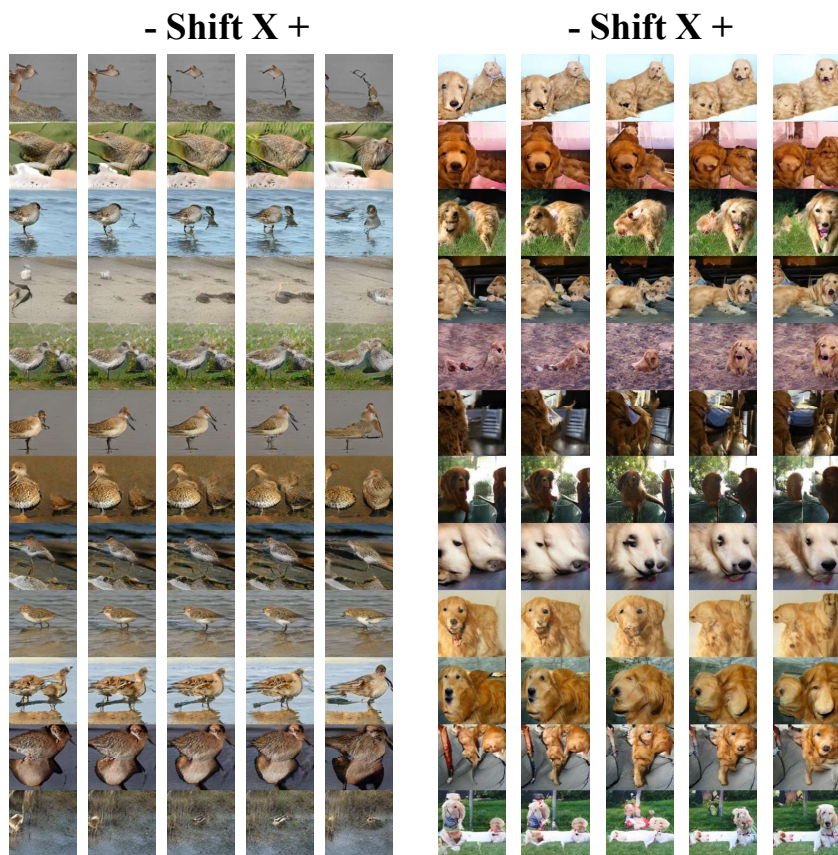


Figure 57: Shift X transformation with DCGAN.

---

#### A.4 ATTRIBUTE TRANSFER

We next provide more attribute transfer examples. Figures 59,60 show pose transfer examples, which are obtained by swapping the part of the latent vector corresponding to scale 1. Figure 61 depict texture transfer examples, which correspond to swapping the parts of the latent vector and the class, corresponding to scales 3,4,5.

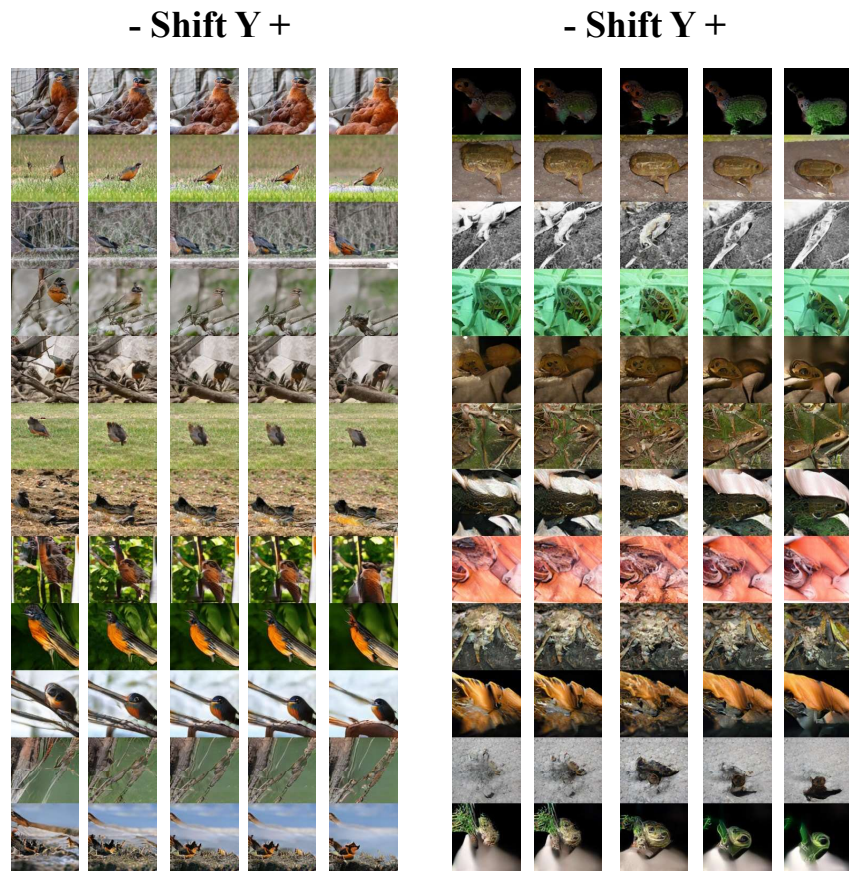


Figure 58: Shift Y transformation with DCGAN.

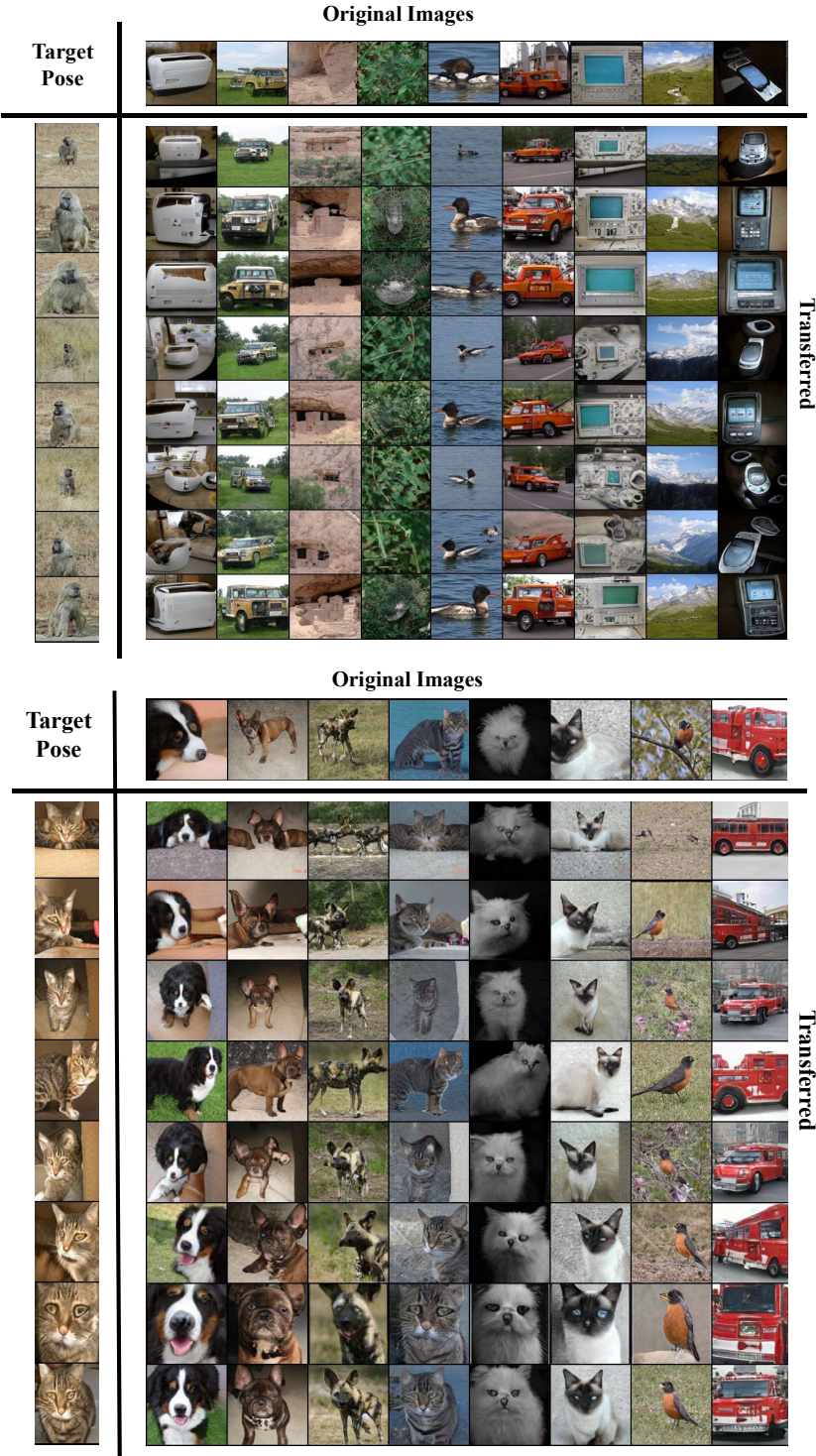


Figure 59: Pose transfer by swapping scale 1 of the latent vector.

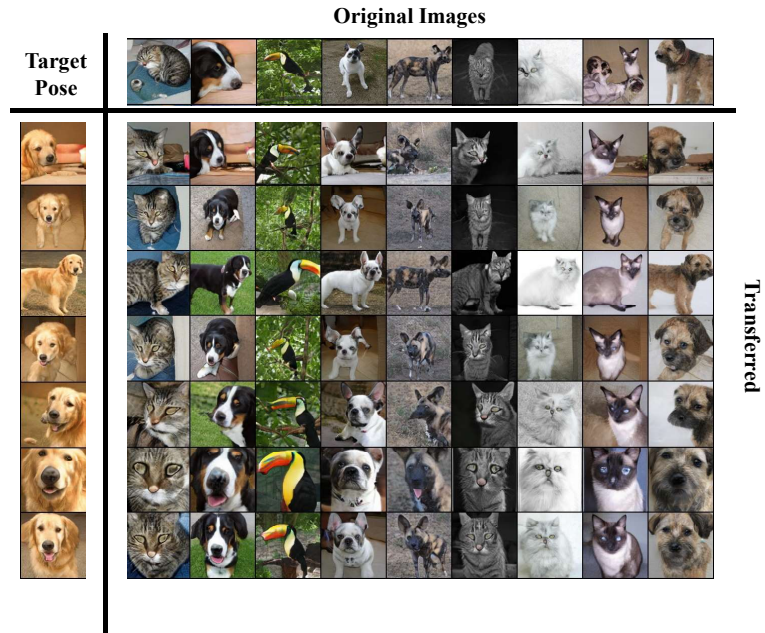


Figure 60: Pose transfer by swapping scale 1 of the latent vector.



Figure 61: Texture transfer by swapping scales 3,4,5 of the latent vector.